Ore Geology Reviews 78 (2016) 85–100

Contents lists available at ScienceDirect

Ore Geology Reviews

journal homepage: www.elsevier.com/locate/oregeorev

Zircon U–Pb, molybdenite Re–Os and muscovite Ar–Ar isotopic dating of the Xitian W–Sn polymetallic deposit, eastern Hunan Province, South China and its geological significance

Xinquan Liang [a,*], Chaoge Dong [a,b], Ying Jiang [a,b], Shichong Wu [c], Yun Zhou [a,d], Haofeng Zhu [c], Jiangang Fu [a,b], Ce Wang [a,b], Yehua Shan [a]

[a] State Key Laboratory of Isotope Geochemistry, Guangzhou Institute of Geochemistry, Chinese Academy of Sciences, Guangzhou 510640, China
[b] University of Chinese Academy of Sciences, Beijing 100049, China
[c] 416 Geological Team, Bureau of Geology and Mineral Exploration and Development of Hunan Province, Zhuzhou 412007, China
[d] College of Earth Sciences, Guilin University of Technology, Guilin, Guangxi 541004, China

ARTICLE INFO

Article history:
Received 23 December 2015
Received in revised form 19 March 2016
Accepted 23 March 2016
Available online 26 March 2016

Keywords:
LA-ICPMS zircon U–Pb dating
Molybdenite Re–Os isotopic dating
Muscovites ^{40}Ar–^{39}Ar dating
Back-arc lithosphere extension
W-Sn polymetallic deposit
Xitian granite complex, Eastern Hunan

ABSTRACT

The Xitian tungsten–tin (W–Sn) polymetallic deposit, located in eastern Hunan Province, South China, is a recently explored region containing one of the largest W–Sn deposits in the Nanling W–Sn metallogenic province. The mineral zones in this deposit comprise skarn, greisen, structurally altered rock and quartz-vein types. The deposit is mainly hosted by Devonian dolomitic limestone at the contact with the Xitian granite complex. The Xitian granite complex consists of Indosinian (Late Triassic, 230–215 Ma) and Yanshanian (Late Jurassic–Early Cretaceous, 165–141 Ma) granites. Zircons from two samples of the Xitian granite dated using laser ablation-inductively coupled mass spectrometer (LA-ICPMS) U–Pb analysis yielded two ages of 225.6 ± 1.3 Ma and 151.8 ± 1.4 Ma, representing the emplacement ages of two episodic intrusions of the Xitian granite complex. Molybdenites separated from ore-bearing quartz-veins yielded a Re–Os isochron age of 149.7 ± 0.9 Ma, in excellent agreement with a weighted mean age of 150.3 ± 0.5 Ma. Two samples of muscovites from ore-bearing greisens yielded $^{40}Ar/^{39}Ar$ plateau ages of 149.5 ± 1.5 Ma and 149.4 ± 1.5 Ma, respectively. These isotopic ages obtained from hydrothermal minerals are slightly younger than the zircon U–Pb age of 151.8 ± 1.4 Ma of the Yanshanian granite in the Xitian area, indicating that the W–Sn mineralization is genetically related to the Late Jurassic magmatism. The Xitian deposit is a good example of the Early Yanshanian regional W–Sn ore-forming event (160–150 Ma) in the Nanling region. The relatively high Re contents (8.7 to 44.0 ppm, average of 30.5 ppm) in molybdenites suggest a mixture of mantle and crustal sources in the genesis of the ore-forming fluids and melts. Based upon previous geochemical studies of Early Yanshanian granite and regional geology, we argue that the Xitian W–Sn polymetallic deposit can be attributed to back-arc lithosphere extension in the region, which was probably triggered by the break-off of the flat-slab of the Palae-Pacific plate beneath the lithosphere.

1. Introduction

China ranks first in the world in terms of tungsten resources and reserves, and has some of the largest tungsten deposits. According to the mineral commodity summaries of the United States Geological Survey (USGS, 2016), China has more than 57% tungsten reserves of the world, and yielded more than 81% of the world's total tungsten production in 2015. The Nanling region in the central part of South China accounts for more than 92% of the Chinese tungsten resource; thus it is the most important Tungsten–Tin (W–Sn) polymetallic province, and it has a close spatial relationship with the Yanshanian granites (Hsü, 1943; Lu, 1986; Mao et al., 2013a, 2013b). Several large-scale W–Sn polymetallic deposits are distributed within the Nanling region, such as the Shizhuyuan, Furong, Yaogangxian, Xihuashan, and Pangushan deposits (Fig. 1). The Shizhuyuan deposit is the largest among the economically important skarn-, greisen- or vein-type W–Sn polymetallic deposits in South China (Mao and Li, 1995; Mao et al., 1995, 1996a, 1996b; Zaw et al., 2007; Yin et al., 2002). It mainly occurs at the contact between the Late Devonian dolomitic limestone and the Late Jurassic (Yanshanian) granitoid, with 750, 000 t WO_3, 490, 000 t Sn, 300, 000 t Bi, 130, 000 t Mo and 200, 000 t Be (Lu et al., 2003). Mining activities have been carried out in the Nanling region for several tens of years, but there remains an untouched reserve of 1.7 million tons of tungsten and 1.2 million tons of tin (Che et al., 2005; Peng et al., 2006; Zaw et al., 2007; USGS, 2016).

* Corresponding author at: Guangzhou Institute of Geochemistry, Chinese Academy of Sciences, No. 511 Kehua Street, Guangzhou 510640, China.
E-mail address: liangxq@gig.ac.cn (X. Liang).

http://dx.doi.org/10.1016/j.oregeorev.2016.03.018
0169-1368/

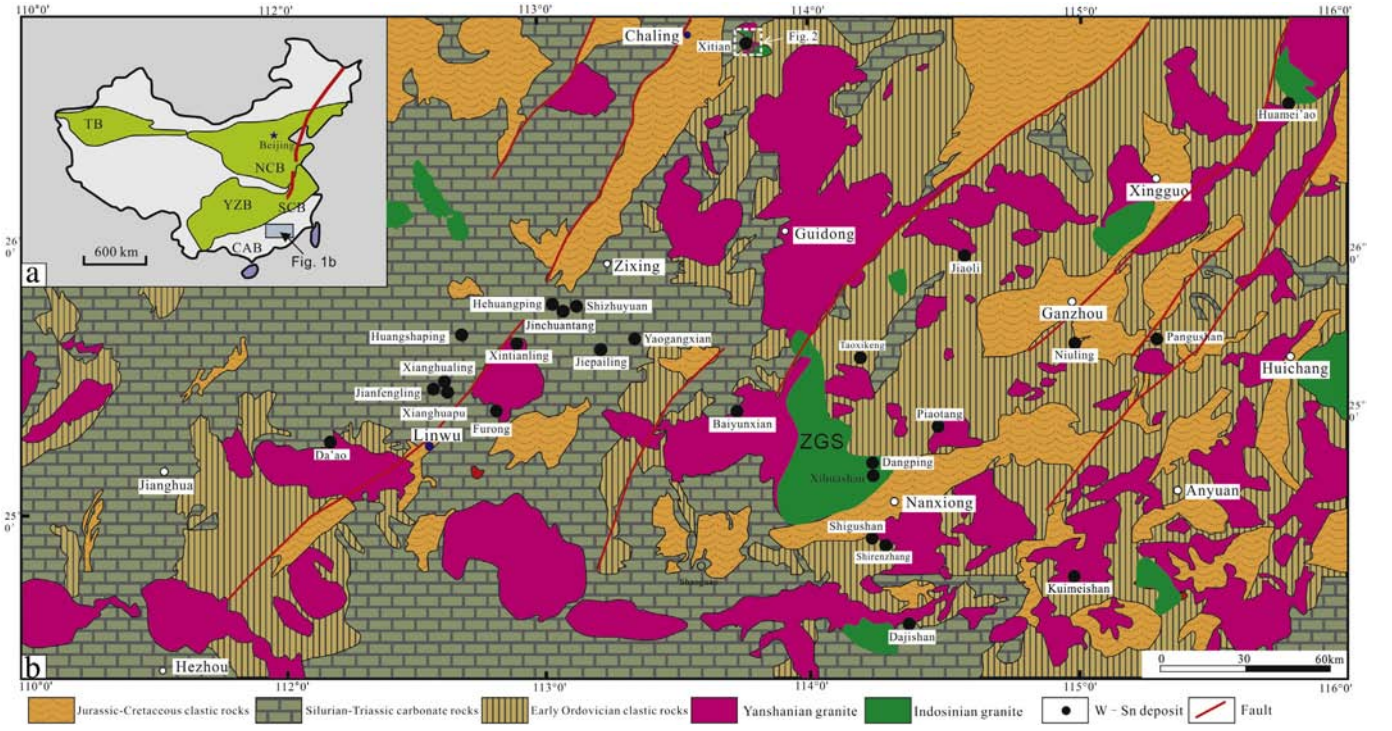

Fig. 1. Sketch map of tungsten and tin deposits in the Nanling region, South China. Modified after Mao et al. (2007) and Zhou et al. (2006). TB–Tarim block; CAB– Cathaysian Block; NCB–North China Block; SCB–South China Block; YZB–Yangtze Block; ZGS–Zhuguangshan.

The Xitian W–Sn polymetallic deposit in eastern Hunan Province is one of the largest newly-discovered deposits during the latest phase of exploration (1999–2011) in the Nanling region, an area with a great potential for W and Sn resources (Wu et al., 2004; Fu et al., 2009, 2012) (Fig. 2). It has four types of mineralization; these are skarn-type hosted at the contact zone between the Yanshanian granite pluton and the Devonian dolomitic limestone, and greisen- and vein-types, as well as structurally altered rocks within or near the Yanshanian granite. The deposit has a Sn reserve of 586,000 tonnes with a grade of 0.26–0.36% and a W reserve of 46,300 tonnes with a WO_3 grade of 0.28–0.63% (Mao et al., 2013a). In addition, Pb, Zn, Mo, Nb and Ta are the by-products from the mineralization (Wu et al., 2004; Luo et al., 2005).

Numerous field investigations, together with geochemical, geochronological, and isotopic studies have been sporadically carried out in the area of the Xitian deposit since 1999 and reported in the Chinese literature (Luo et al., 2005; Ma et al., 2005; Zeng et al., 2005; Cai and Jia, 2006; Xu et al., 2006; Chen et al., 2013; Zhou et al., 2013; Niu et al., 2015; Deng et al., 2015). Various geochronologic techniques have been adopted in the studies, including the K–Ar, Rb–Sr, Sm–Nd isochrons, and LA-ICPMS, SHRIMP, and SIMS zircon U–Pb. However, the lack of systematic application of modern techniques has resulted in a limited consensus on the exact timing of the granitic intrusion, although it has been tentatively dated between 175-161 Ma by regional petrographic correlation (HNBGMR, 1988). The intrusion has been subdivided into two stages, 233–227 Ma and 155–150 Ma (Ma et al., 2005; Niu et al., 2015; Su et al., 2015), and three stages, at ~230 Ma or Indosinian, at ~155 Ma or Early Yanshanian, and ~114 Ma (Whole rock Rb-Sr dating) or Late Yanshanian (Chen et al., 2014; Fu et al., 2009). How the Xitian deposit relates to these stages is a matter of debate. A combination of molybdenite Re–Os, muscovite Ar–Ar, and fluid inclusion Rb–Sr dating (Liu et al., 2008a, 2008b; Fu et al., 2009, 2012; Wu et al., 2012; Wang et al., 2015) has yielded an age of 157–150 Ma or Late Jurassic for the deposit. However, Niu et al. (2015) argued the presence of another mineralization in 227–233 Ma, and Deng et al. (2015) even obtained a molybdenite Re–Os age of 225.5 ± 3.6 Ma. It is therefore necessary to undertake a systematic study to date the deposit and the adjacent granite to resolve this conundrum.

This paper aims to accurately date the Xitian W–Sn deposit and the associated granites. Zircon U–Pb, molybdenite Re–Os and muscovite Ar–Ar isotopic dating, together with field, petrographic and geochemical studies, have rigorously been carried out in these years. These data confirm the two stages of the Xitian granitic intrusion and, what is more, the temporal relationship between the deposit and the Early Yanshanian magmatism. This is helpful in better understanding the W–Sn mineralization of the Nanling region. The new data are combined with recently published geochronology of other W–Sn deposits in the Nanling region to accurately and precisely constrain the timing of mineralization and to identify the geodynamic processes that contraolled the metallogenesis.

2. Regional geology

The South China Block (SCB) is composed of the Yangtze Block (YZB) to the west and the Cathaysian Block (CAB) to the east (Fig. 1a), which amalgamated during the Neoproterozoic Sibao (also called "Jiangnan" or "Jinning") orogeny (Chen and Jahn, 1998; Li, 1998a, 1998b; Zhao et al., 2011). The YZB comprises Neo-Archean metamorphosed basement, sporadically exposed in Yunnan, Guizhou, and Hubei provinces (Gao et al., 1999; Qiu et al., 2000; Charvet, 2013). The CAB is composed of Proterozoic basement, Sinian to Triassic sedimentary cover (Li et al., 1997, 2012; Chen and Jahn, 1998; Yu et al., 2009), and Mesozoic granitoid intrusions and volcanic rocks with a total area of ~220,000 km^2, characterized by extensive metallic mineralization (Zhou et al., 2006). The Nanling region, geologically located in the northwestern part of the CAB, is an important W–Sn–Mo–Bi–Pb–Zn–U metallogenic belt where the Xitian W-Sn polymetallic deposit is in the north (Fig. 1b). It comprises two Caledonian units, the southern Hunan–eastern Guangxi–northern Guangdong depression in the west and the southern Hunan–southern Jiangxi–Guangdong uplift in the east.

Late Mesozoic (Jurassic or Early Yanshanian) granites are distributed throughout much of the Nanling region, whereas Early Mesozoic (Indosinian) granitoid intrusions are located mainly in the region of the Zhuguangshan mountains (Fig. 1) (Li, 2000; Wang et al., 2003a,

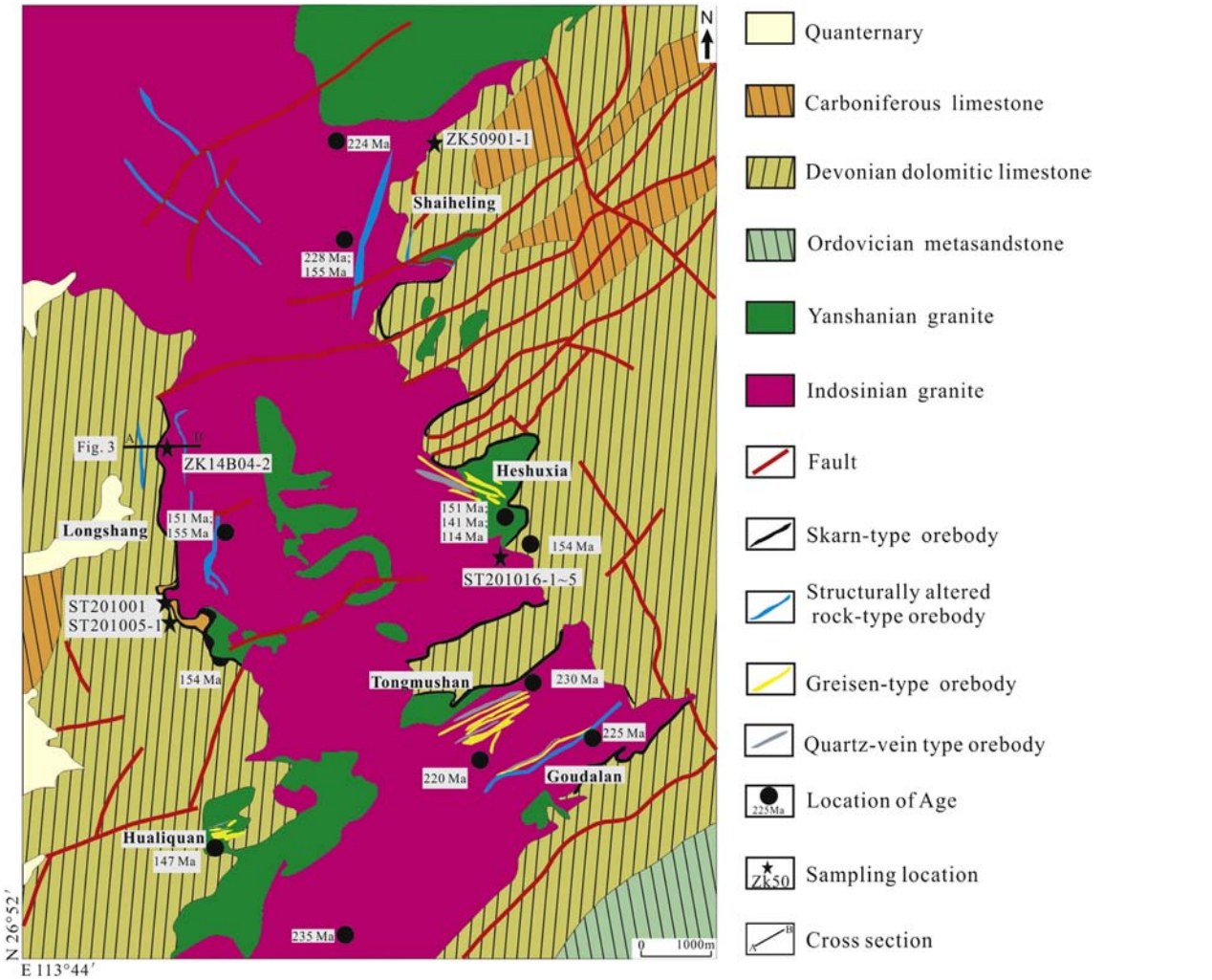

Fig. 2. Schematic geological map of the Xitian W–Sn deposit. Modified after Wu et al. (2004). Age data from Chen et al. (2013); Fu et al. (2012) and Liu et al. (2008a).

2003b, 2007; Zhou et al., 2006; Li and Li, 2007; Niu et al., 2015). Nearly all of the polymetallic tungsten and tin deposits in South China are associated with Late Mesozoic granites, and are located at the endo- and exo-contacts of granitic intrusions (Mao and Li, 1995; Mao et al., 1995, 1996a, 1996b; Zaw et al., 2007; Yin et al., 2002; Wang et al., 2008; Guo et al., 2011, 2014). The Yanshanian plutons consist predominantly of seriate or porphyritic monzogranites, composed of quartz (25–30%), K-feldspar and plagioclase (25–45%) with a K-feldspar/plagioclase ratio of >1, and minor biotite (Fu et al., 2004a, 2004b; Li et al., 2004; Zhu et al., 2005; Zhang et al., 2006; Wei et al., 2007; Yao et al., 2007; Yang et al., 2009a, 2009b; Guo et al., 2011; Zhou et al., 2015). Accessory minerals comprise tantalite, ilmenite, wolframite, cassiterite, molybdenite, apatite, titanite, magnetite, zircon and fluorite. The geochemical features of the granites are SiO_2 >65%, with an alkaline content of >8%, K_2O>Na_2O, and A/CNK>1.1, thus indicative of calcalkaline granites (Luo et al., 2005; Li et al., 2007b, 2007c, 2007d, 2007e; Guo et al., 2011).

The Early Yanshanian granitoids consist mainly of slightly peraluminous biotite monzogranites and K-feldspar granites, which are closely associated in time and space with subordinate amphibole-bearing granites, and muscovite- and garnet-bearing granites (Li et al., 2007b). Biotite-bearing monzogranites are previously considered as crustal transformation-type or S-type granites originated from regional Paleoproterozoic meta-sedimentary rocks that occur in the region (RGNTD, 1985; Li, 1991; Li et al., 2007b). However, some of them are recently classified as fractionationed I-type granites or A-type granites (Zhou and Li, 2000; Ma et al., 2004; Fu et al., 2004a; Bai et al., 2005; Jiang et al., 2005, 2006, 2009, 2011; Li et al., 2007e, 2014a; Huang et al., 2011; Zhou et al., 2013). All these rocks constitute melts generated in an anorogenic, intraplate environment where regional lithospheric extension occurred in the Early Yanshanian (Li et al., 2007b; Jiang et al., 2009, 2011; Zhou et al., 2013).

The W–Sn mineralization in the region consists of four major types: greisen-, skarn-, quartz vein- and structurally altered rock-types. These types are present either in all in most deposits, or individually in some deposits, for example, the Dengfuxian and Xihuashan quartz vein-type deposits (Cai et al., 2012; Wang et al., 2011a; Hu et al., 2012b). Besides, minor types include stratiform cassiterite + sulfide-, altered granite-, and stockwork-types (Feng et al., 2011; Niu et al., 2015). All of these types are spatially associated with widespread Late Jurassic granitic intrusions, as they frequently occur at the contacts between the intrusions and sedimentary strata, and are hosted by Devonian to Permian sedimentary rocks and/or granites. Field observations seem to reveal a nearly similar age for the deposits and the associated granites (e.g. Mao et al., 2004a, 2004b, 2013a, 2013b; Guo et al., 2011, 2014; Wang et al., 2011a, 2011b; Hu et al., 2012a, 2012b; Li et al., 2014b).

3. Geology of the Xitian deposit

The Xitian W–Sn polymetallic deposit is located within the Chaling–Chenzhou deep fault, a major regional-scale structure, whose activity is presumably related to the formation of the deposits (Wang et al., 2003a;

Wu et al., 2004) (Fig. 1b). It is an S–N-trending extensional granite dome, surrounded by Paleozoic sedimentary rocks that were deformed into a series of NE-trending folds and NE- or NEE-trending strike-slip faults (Wu et al., 2012). These folds with a steeply NE-dipping axial plane formed during the Indosinian orogeny (HNBGMR, 1988; Fig. 2). They include the Shaiheling and Heshuxia synclines at the eastern side of the dome, and the Longshang syncline at the western side. Faults terminate at or cut across the contact, seem to control the W–Sn ore bodies of the deposit.

Surrounding the magmatic dome are Ordovician, Devonian and Carboniferous sedimentary rocks (Fig. 2). The Ordovician strata in the south comprise neritic facies sandstones and siltstones, and are overlain unconformably by the Devonian strata. The Devonian strata are subdivided into two formations, the Middle Devonian Qiziqiao Formation and the Upper Devonian Xikuangshan Formation (HNBGMR, 1988). Both consist of impure carbonate rocks, with an appreciable amount of clay, which have a high content of W and Sn with respect to the corresponding Clarke values (Wu et al., 2004). In the folds comprising these strata, axial cleavages and secondary fractures are so densely developed that they might have provided channels for ore-forming fluids.

The type of mineralization in skarn seems to vary with the formation at the contact. For example, W-Sn mineralization tends to occur in the Qiziqiao Formation, and Sn mineralization in the Xikuangshan Formation (Wu et al., 2004; Luo et al., 2005).

The Xitian granite complex, with an area of ca. 240 km^2 and in an N–S-trending dumbbell shape, makes up the majority of the dome. As mentioned above, it comprises two distinctive phases of granitic intrusion: Indosinian and Early Yanshanian. The Indosinian granites cover 60% area of the granite complex, in the form of batholith and stocks, and are mainly composed of grayish-white, coarse- to medium-grained porphyritic biotite monzogranite and K-feldspar granite (Ma et al., 2004; Fu et al., 2009; Niu et al., 2015). They have a porphyritic and coarse-grained granitic texture, where unequal crystals are frequently aligned around the contact to make up flow foliation (Ni et al., 2014). They have 10–15% K-feldspar phenocrysts embedded in the matrix of 24–36% quartz, 23–40% K-feldspar, 25–45% plagioclase, and 3–10% biotite (Fu et al., 2009) (Fig. 3a-b). Accessory minerals include magnetite, ilmenite, tourmaline, apatite and zircon. Dark mafic microgranular enclaves are very common. The measured ages of the granites have a range of 233 Ma to 215 Ma (Ma et al., 2005; Fu et al., 2009; Chen et al., 2013; Yao et al., 2013; Niu et al., 2015).

The Early Yanshanian granites consist of grayish white, fine- and medium-grained porphyritic biotite monzogranite and hornblende-bearing biotite granite, in the form of stocks, apophyses and bosses. They are fine-grained, with or without porphyritic texture. They are composed of 28–30% quartz, 28–38% K-feldspar, 25–30% plagioclase, 5–12% biotite and minor muscovite (Fu et al., 2009; Zhou et al., 2013, 2015; Fig. 3c-d). Accessory minerals are magnetite, tourmaline, topaz, apatite and zircon. These granites have a smaller size and a smaller content of phenocrysts and a greater content of quartz, muscovite and fluorite than the Indosinian granites. They have previously been dated as 165–147 Ma (Liu et al., 2008a; Fu et al., 2012; Chen et al., 2013; Yao et al., 2013; Zhou et al., 2013, 2015).

In the Xitian deposit, more than 100 W–Sn polymetallic ore bodies are divided into four major types of W–Sn mineralization: skarn-, greisen-, quartz vein- and structurally altered rock-types (Fig. 2). Skarns are present only in the Longshang, Shaiheling and Heshuxia mining districts, and occur in the endo- and exo-contact zones between the Devonian limestone and the Xitian Yanshanian granite pluton (Wu et al., 2004, 2012; Fu et al., 2009). The majority of them have an N–S, NE or NEE trend and a W, SE or SSE dip direction,

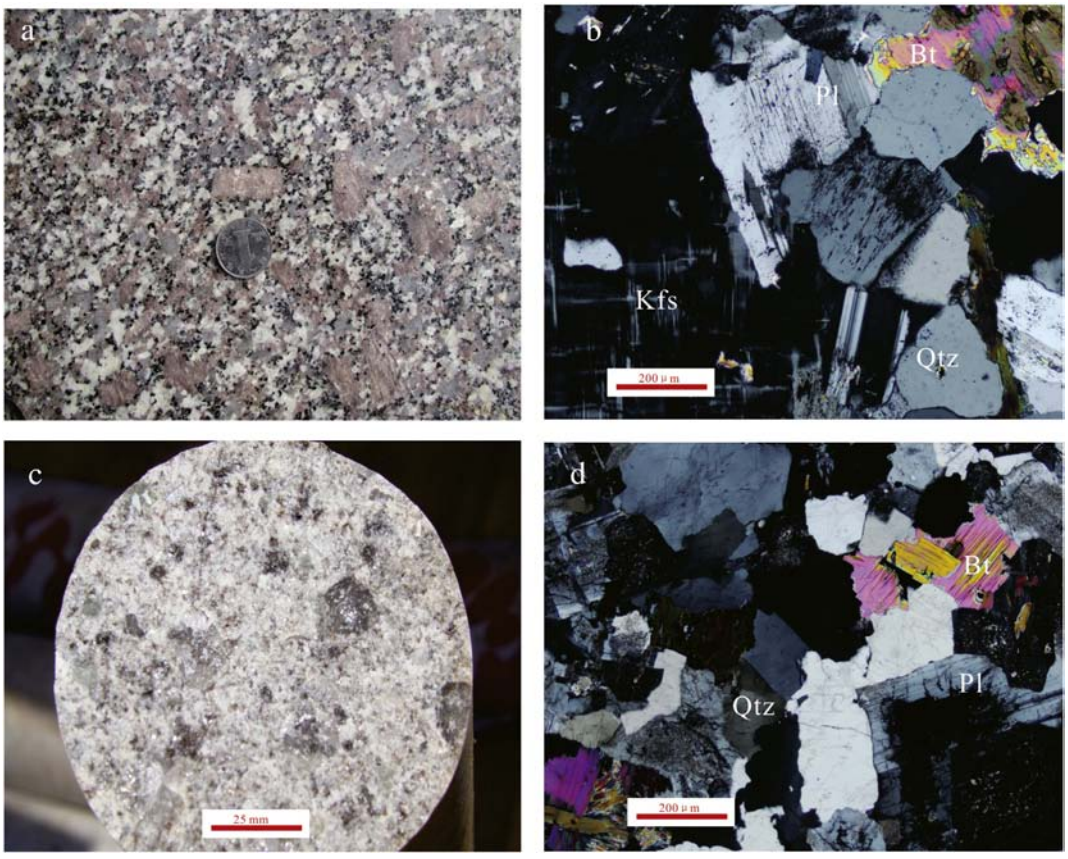

Fig. 3. Hand specimens and microscopic images of the granitoids from the Xitian deposit. (a, b): the coarse-grained porphyritic biotite K-feldspar granite; (c, d): the fine-grained porphyritic biotite granite. Bt–Biotite; Kfs– K-feldspar; Pl–plagioclase; Qtz–Quartz.

and are hosted by Devonian sedimentary rocks. They are 400–4,500 m in length and 4.2 m in average vertical thickness, with an average ore grade of 0.27% WO_3 and 0.43% Sn (Wu et al., 2012). Ore minerals include cassiterite, scheelite, chalcopyrite and pyrite, with a minor amount of christophite, magnetite and pyrrhotite. Gangue minerals are diopside, epidote, quartz, feldspar, calcite, and so forth.

Greisen-type ore bodies are present in the Heshuxia, Tongmushan, Dagoulan and Hualiquan mining districts (Wu et al., 2012; Fig. 2). Most of them trend toward ENE or NW, and dip toward SSE or NE. They are hosted by Early Yanshanian granites. They are 100–1,000 m in length and 0.5 –3.0 m in width, with an ore grade of 0.16–3.35 % Sn and 0.17–2.08 % WO_3 (Wu et al., 2012). Ore minerals are sphalerite, pyrite, cassiterite, scheelite, wolframite, molybdenite, bismuthinite and chalcopyrite. Gangue minerals are quartz, muscovite and minor topaz.

Structurally altered rock–type ore bodies are strictly controlled by the fracture zones in the Xitian granites and/or the Devonian sandstone. They cut across the skarn- and greisen-type ore bodies (Fu et al., 2012; Wu et al., 2012), indicating a younger age for them. Most of them have an NE or E–W trend and an SE or S dip direction. They are 500–2,700 m in length and 0.8–10.0 m in width, with an average ore grade of 0.27% Sn and 0.44% WO_3 (Luo et al., 2005; Liu et al., 2008a; Fu et al., 2012; Wu et al., 2012). Ore minerals consist of sphalerite, galena and pyrite with minor amounts of cassiterite and arsenopyrite. Gangue minerals comprise feldspar, quartz and chlorite (Yang et al., 2007).

Quartz vein–type ore bodies exist in the Hualiquan, Goudalan and Tongmushan mining districts, and are controlled by joints. They are generally 0.5 m wide and no more than 1 m in width (Wu et al., 2012). Ore minerals are wolframite, sphalerite, pyrite, arsenopyrite, molybdenite and chalcopyrite. Gangue minerals are quartz, feldspar, muscovite and minor topaz (Fu et al., 2012).

4. Sampling and analytical procedures

4.1. Zircon U–Pb dating

Two samples were chosen for U-Pb dating. The sample from drill core ZK50901-1 is a coarse-grained porphyritic biotite K-feldspar granite (Fig. 3a) and the sample from ZK14B04-2 is a fine-grained porphyritic biotite granite (Fig. 3c). The first sample was collected at a depth of 250-253 m in the Shaiheling mining district (Fig. 2), and the second sample at a depth of 198-200 m in the Longshang mining district (Figs. 2 and 4).

Zircons were separated by conventional heavy liquid and magnetic methods, and then handpicked under a binocular microscope. The separated grains were mounted in epoxy resin and polished to get a cross-section for exposing the central feature of the zircons. Reflected and transmitted light photomicrographs and cathodoluminescence (CL) images (Fig. 5) were taken to determine the internal structures of the zircon grains. U–Pb dating and trace element analyses were carried out at the State Key Laboratory of Isotope Geochemistry, Guangzhou Institute of Geochemistry, Chinese Academy of Sciences, using a LA-ICPMS equipped with a Resonetics Resolution M-50 (193 nm ArF excimer) laser system. Sample mounts were placed in a specially designed double volume sample cell flushed with Ar and He. Laser ablation was conducted at a constant energy (between 80 and 81 mJ cm^{-3}) at 10 Hz. The analysis spots were 31 μm in diameter. The ablated material was carried by He–Ar gas via a custom-made Squid system to homogenize the signal to the ICPMS (Liang et al., 2009). Raw data were processed using a time-drift correction and quantitative calibration and U–Pb dating were established using an in-house program ICPMSDataCal (Liu et al., 2010). External standard glass NIST SRM 610 (Pearce et al., 1997; Gao et al., 2002) and standard zircon Temora (Black et al., 2003) were used for external calibration. ^{29}Si was used as the internal standard. A

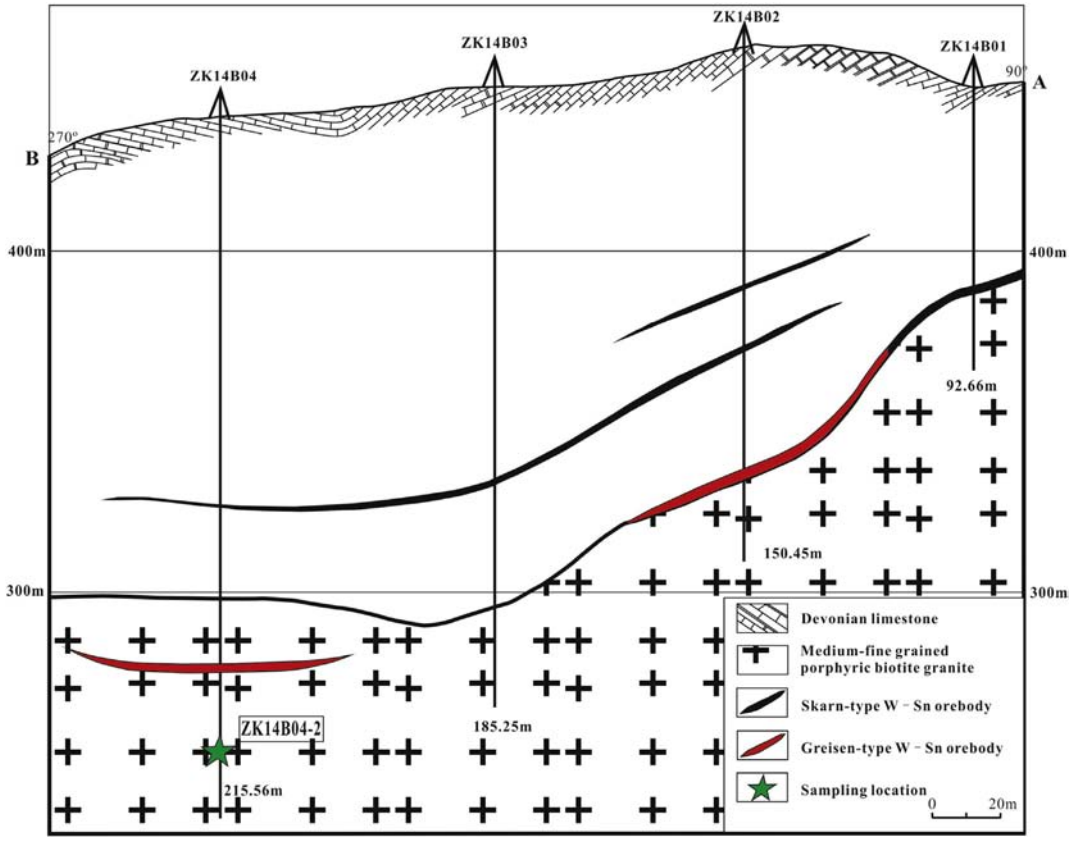

Fig. 4. Section number 14B showing the geology based on surface geology and drilling of the Xitian deposit. The location of sample ZK14B04-2 is shown.

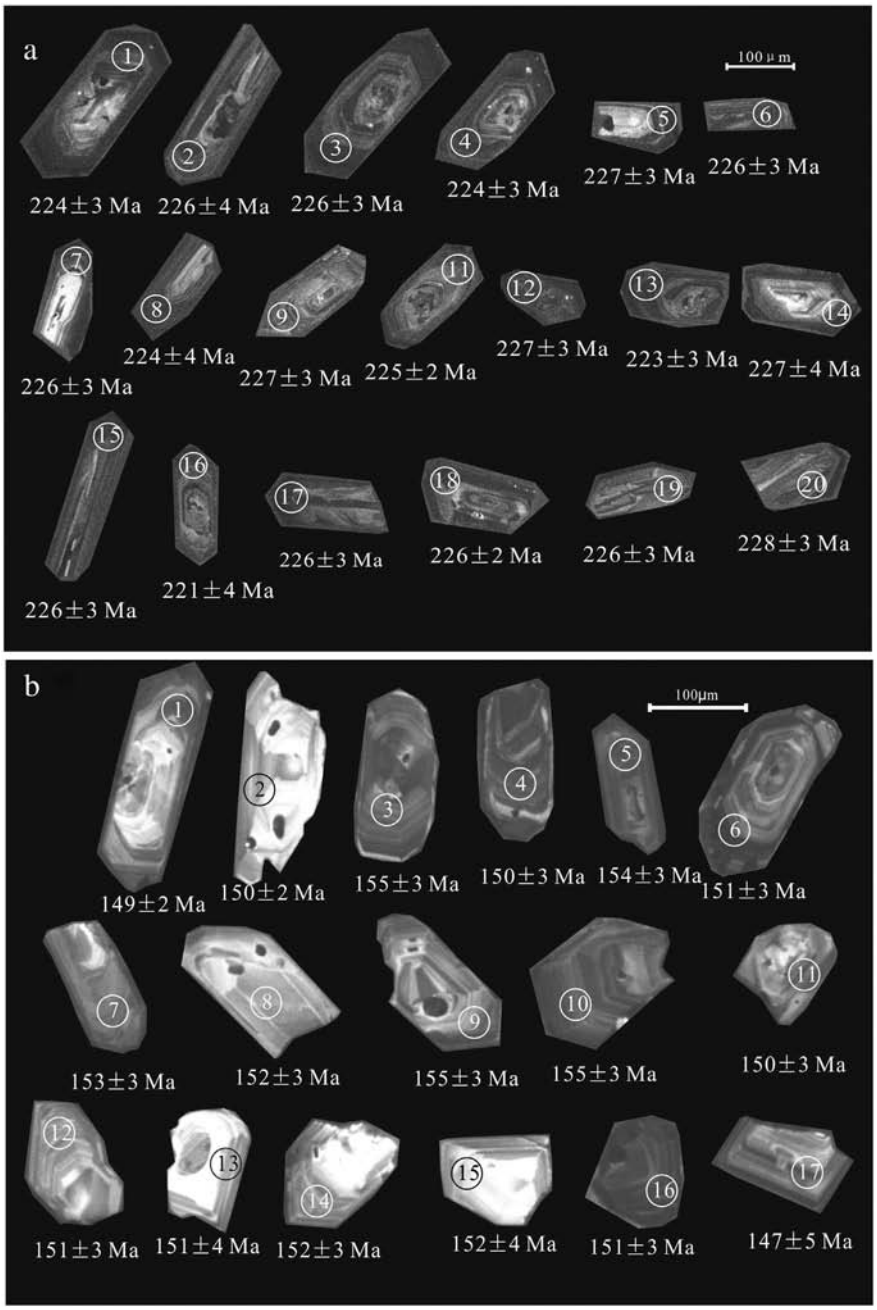

Fig. 5. Cathodoluminescence (CL) images showing internal features of zircons from the coarse-grained porphyritic K-feldspar granite (ZK50901-1, a) and the fine-grained porphyritic biotite granite (ZK14B04-2, b).

common Pb correction and ages of the samples were carried out using the EXEL program of ComPbCorr#3-17 (Andersen, 2002). Concordia diagrams and weighted mean calculations were made using the ISOPLOT program (version 3.0; Ludwig, 2003).

4.2. Molybdenite Re–Os dating

Five samples of molybdenite were collected for Re–Os dating from wolframite -bearing quartz veins in the Xitian deposit (Fig. 2). The ore-bearing quartz veins consist of quartz, wolframite, molybdenite and muscovite; and the molybdenite displays a flake-like texture along the margins of the veins. The samples were crushed in an agate mortar, and then molybdenite grains for Re–Os dating were handpicked under binocular microscope to remove the impurities (purity >99%). The Re–Os isotope analysis was performed using an inductively coupled plasma mass spectrometer (ICPMS) in the State Key Laboratory of Isotope Geochemistry, Guangzhou Institute of Geochemistry, Chinese Academy of Sciences, China. The Carius tubes method was used to digest samples (Shirey and Walker, 1995), and Re and Os were separated using the distillation technique described in Du et al. (2004). Details of the chemical procedure were described by Sun et al. (2001, 2010).

The average blanks for Re and Os are 2.8 pg and 0.7 pg, respectively. These blanks have negligible effect on the measured Re and Os abundances. The analytical reliability was tested by repeated analyses of the molybdenite standard HLP-5, which is a carbonate rock vein–type molybdenum–lead deposit in the Jinduicheng–Huanglongpu area of Shanxi Province, China (Sun et al., 2001, 2010). The uncertainty in each individual age determination was about 0.35% including the uncertainty of the decay constant of ^{187}Re, uncertainty in isotope ratio measurement, and spike calibrations. The average Re–Os age for HLP-5 is

221.3 ± 0.3 Ma with confidence limit of 95% (Stein et al., 1997). Median age and mean absolute deviation were 221.34 ± 0.12 Ma. The average Re concentration was 283.71 ± 1.54 ppb. The average Os concentration was 657.95 ± 4.74 ppb. Molybdenite model ages were calculated using a ^{187}Re decay constant of 1.666×10^{-11} per year (Smoliar et al., 1996), following the equation $t = [\ln(1 + {}^{187}Os/{}^{187}Re)]/\lambda$, where λ is the decay constant of ^{187}Re.

4.3. Muscovite ^{40}Ar–^{39}Ar dating

Two samples of greisens or greisenized granites were collected (Fig. 2), from which muscovite was seperated. The separates were then washed repeatedly in an ultrasonic bath using deionized water and acetone. About 10 mg aliquots were wrapped in Al foil and stacked in quartz vials. After samples had been stacked, the sealed quartz vials were put in a quartz canister, which was wrapped with cadmium foil (0.5 mm in thickness) to act as a slow neutron shield thereby preventing interface reactions during irradiation. Samples were irradiated for 48 hours in channel B4 of Beijing 49-2 reactor at the Chinese Academy of Nuclear Energy Sciences. During irradiation, the vials were rotated at a speed of two cycles per minute to ensure uniformity of the irradiation. The biotite standard ZBH-2506 (132.5 Ma) was used to monitor the neutron flux. $^{40}Ar/^{39}Ar$ stepwise heating analyses were performed at the Argon Laboratory of the State Key Laboratory of Isotope Geochemistry, Guangzhou Institute of Geochemistry, Chinese Academy of Sciences, using a GVI5400 mass spectrometer equipped with a Faraday cup and an ion counter (multiplier) for Ar isotopes measurement. The irradiated samples were loaded into a sample holder and degassed at 200–250°C for about 72 hours in a high vacuum system. The samples were analyzed in 16 temperature steps from 780°C to total fusion at 1480–1500°C. Step-heating analysis was carried out in a double-vacuum resistance furnace. Samples were heated at each temperature step for 10 min and the extracted gasses purified using two SAES Zr–Al getters (NP10). K_2SO_4 and CaF_2 crystals were analyzed to calculate Ca, K correction factors: $({}^{39}Ar/{}^{37}Ar)_{Ca} = 8.984 \times 10^{-4}$, $({}^{36}Ar/{}^{37}Ar)_{Ca} = 2.673 \times 10^{-4}$, $({}^{40}Ar/{}^{39}Ar)_{K} = 5.97 \times 10^{-3}$. The data–processing software we used was the ArArCALC 2.4 software by Koppers (2002). The plateau criteria involves: (1) at least 60% of the ^{39}Ar released in three or more contiguous steps, and the ages of these steps have to be concordant within 1 sigma error; (2) no resolvable slope on the plateau; (3) no outliers or trends at the upper or lower steps; and (4) probability of fit of the plateau is >0.01.

5. Results

5.1. Zircon U–Pb ages

Zircon CL images of the Xitian granite are displayed in Fig. 5. In the images, most of the zircons are transparent, euhedral and prismatic, and have an oscillatory zoning or linear zoning, diagnostic of magmatic origin (Corfu et al., 2003). They are generally colorless or light brown and 80–270 μm long, with a length/width ratio of 1.1–2.6.

Table 1
Zircon U–Pb dating results of granite in the Xitian W–Sn deposit.

Analysed spot	Concentration		Th/U	Isotopic ratios and 1σ errors						Corrected ages and ±1σ errors (Ma)					
	^{232}Th	^{238}U		$^{207}Pb/^{206}Pb$	1σ	$^{207}Pb/^{235}U$	1σ	$^{206}Pb/^{238}U$	1σ	$^{207}Pb/^{206}Pb$	1σ	$^{207}Pb/^{235}U$	1σ	$^{206}Pb/^{238}U$	1σ
ZK50901-1 coarse-grained porphyritic biotite K-feldspar granite															
ZK50901-1-01	754	1288	0.59	0.05638	0.00174	0.28051	0.00864	0.03601	0.00046	477.8	100.9	251.1	6.9	228.1	2.8
ZK50901-1-02	428	2941	0.15	0.05528	0.00231	0.26690	0.01246	0.03488	0.00058	433.4	97.2	240.2	10.0	221.0	3.6
ZK50901-1-03	611	1726	0.35	0.05515	0.00184	0.27305	0.00926	0.03563	0.00044	416.7	78.7	245.1	7.4	225.7	2.7
ZK50901-1-04	1330	2866	0.46	0.05495	0.00158	0.27428	0.00788	0.03562	0.00035	409.3	64.8	246.1	6.3	225.6	2.2
ZK50901-1-05	619	2199	0.28	0.05461	0.00175	0.27482	0.00876	0.03565	0.00055	394.5	70.4	246.5	7.0	225.8	3.4
ZK50901-1-06	2833	3941	0.72	0.05374	0.00167	0.26638	0.00813	0.03527	0.00042	361.2	70.4	239.8	6.5	223.5	2.6
ZK50901-1-07	547	1184	0.46	0.05474	0.00219	0.27187	0.01129	0.03576	0.00058	466.7	88.9	244.2	9.0	226.5	3.6
ZK50901-1-08	717	390	1.84	0.05506	0.00243	0.27219	0.01197	0.03568	0.00046	413.0	93.5	244.4	9.6	226.0	2.9
ZK50901-1-09	658	447	1.47	0.05352	0.00237	0.26718	0.01197	0.03583	0.00050	350.1	100.0	240.4	9.6	226.9	3.1
ZK50901-1-11	483	1966	0.25	0.05263	0.00156	0.26259	0.00800	0.03556	0.00040	322.3	73.1	236.8	6.4	225.2	2.5
ZK50901-1-12	1840	1793	1.03	0.05078	0.00155	0.25488	0.00827	0.03565	0.00053	231.6	67.6	230.5	6.7	225.8	3.3
ZK50901-1-13	505	2122	0.24	0.05193	0.00170	0.25456	0.00824	0.03539	0.00057	283.4	74.1	230.3	6.7	224.2	3.6
ZK50901-1-14	720	846	0.85	0.05128	0.00205	0.25799	0.01068	0.03587	0.00054	253.8	88.0	233.0	8.6	227.2	3.4
ZK50901-1-15	4286	2726	1.57	0.05015	0.00203	0.25368	0.00990	0.03564	0.00048	211.2	97.2	229.6	8.0	225.7	3.0
ZK50901-1-16	514	1565	0.33	0.04849	0.00164	0.24275	0.00808	0.03542	0.00048	124.2	84.2	220.7	6.6	224.4	3.0
ZK50901-1-17	284	1631	0.17	0.04841	0.00166	0.24578	0.00883	0.03581	0.00041	120.5	81.5	223.1	7.2	226.8	2.6
ZK50901-1-18	923	810	1.14	0.05105	0.00213	0.25523	0.01082	0.03572	0.00052	242.7	100.9	230.8	8.8	226.3	3.2
ZK50901-1-19	1088	5303	0.21	0.04971	0.00162	0.24496	0.00773	0.03528	0.00054	189.0	75.9	222.5	6.3	223.5	3.4
ZK50901-1-20	103	939	0.11	0.04981	0.00208	0.24837	0.01023	0.03573	0.00065	187.1	96.3	225.3	8.3	226.3	4.0
ZK14B04-2 fine-grained porphyritic biotite granite															
ZK14B04-2-1	303	658	0.46	0.04772	0.00287	0.15503	0.00972	0.02346	0.00035	87.1	146.3	146.3	8.5	149.5	2.2
ZK14B04-2-2	480	875	0.55	0.04667	0.00234	0.15152	0.00778	0.02350	0.00038	31.6	118.5	143.3	6.9	149.7	2.4
ZK14B04-2-3	287	566	0.51	0.04654	0.00467	0.15875	0.01825	0.02440	0.00048	33.4	216.6	149.6	16.0	155.4	3.0
ZK14B04-2-4	345	1273	0.27	0.04753	0.00267	0.15485	0.00853	0.02348	0.00047	76.0	135.2	146.2	7.5	149.6	3.0
ZK14B04-2-5	383	837	0.46	0.04614	0.00362	0.15632	0.01199	0.02423	0.00043	400.1	-216.6	147.5	10.5	154.3	2.7
ZK14B04-2-6	325	713	0.46	0.04728	0.00366	0.15518	0.01164	0.02367	0.00046	64.9	174.0	146.5	10.2	150.8	2.9
ZK14B04-2-7	155	291	0.53	0.04671	0.00523	0.15917	0.01872	0.02405	0.00052	35.3	248.1	150.0	16.4	153.2	3.3
ZK14B04-2-8	175	335	0.52	0.04822	0.00354	0.16105	0.01244	0.02393	0.00053	109.4	166.6	151.6	10.9	152.4	3.4
ZK14B04-2-9	363	716	0.51	0.05149	0.00361	0.17376	0.01231	0.02441	0.00040	261.2	158.3	162.7	10.7	155.5	2.5
ZK14B04-2-10	208	378	0.55	0.05238	0.00496	0.17396	0.01546	0.02441	0.00049	301.9	213.9	162.8	13.4	155.4	3.1
ZK14B04-2-11	192	255	0.75	0.05219	0.00585	0.16662	0.01816	0.02350	0.00053	294.5	257.4	156.5	15.8	149.8	3.3
ZK14B04-2-12	387	483	0.80	0.05100	0.00393	0.16609	0.01271	0.02371	0.00047	242.7	177.8	156.0	11.1	151.1	2.9
ZK14B04-2-13	143	205	0.70	0.04751	0.00653	0.15368	0.02354	0.02373	0.00062	76.0	296.3	145.2	20.7	151.2	3.9
ZK14B04-2-14	236	509	0.46	0.04981	0.00348	0.16461	0.01205	0.02384	0.00047	187.1	164.8	154.7	10.5	151.9	3.0
ZK14B04-2-15	97	180	0.54	0.05010	0.00605	0.15577	0.01791	0.02387	0.00062	198.2	259.2	147.0	15.7	152.1	3.9
ZK14B04-2-16	237	747	0.32	0.04605	0.00298	0.15569	0.01191	0.02368	0.00043	400.1	-250.0	146.9	10.5	150.9	2.7
ZK14B04-2-17	91	162	0.56	0.05056	0.00888	0.15604	0.02472	0.02304	0.00082	220.4	362.9	147.2	21.7	148.9	3.2

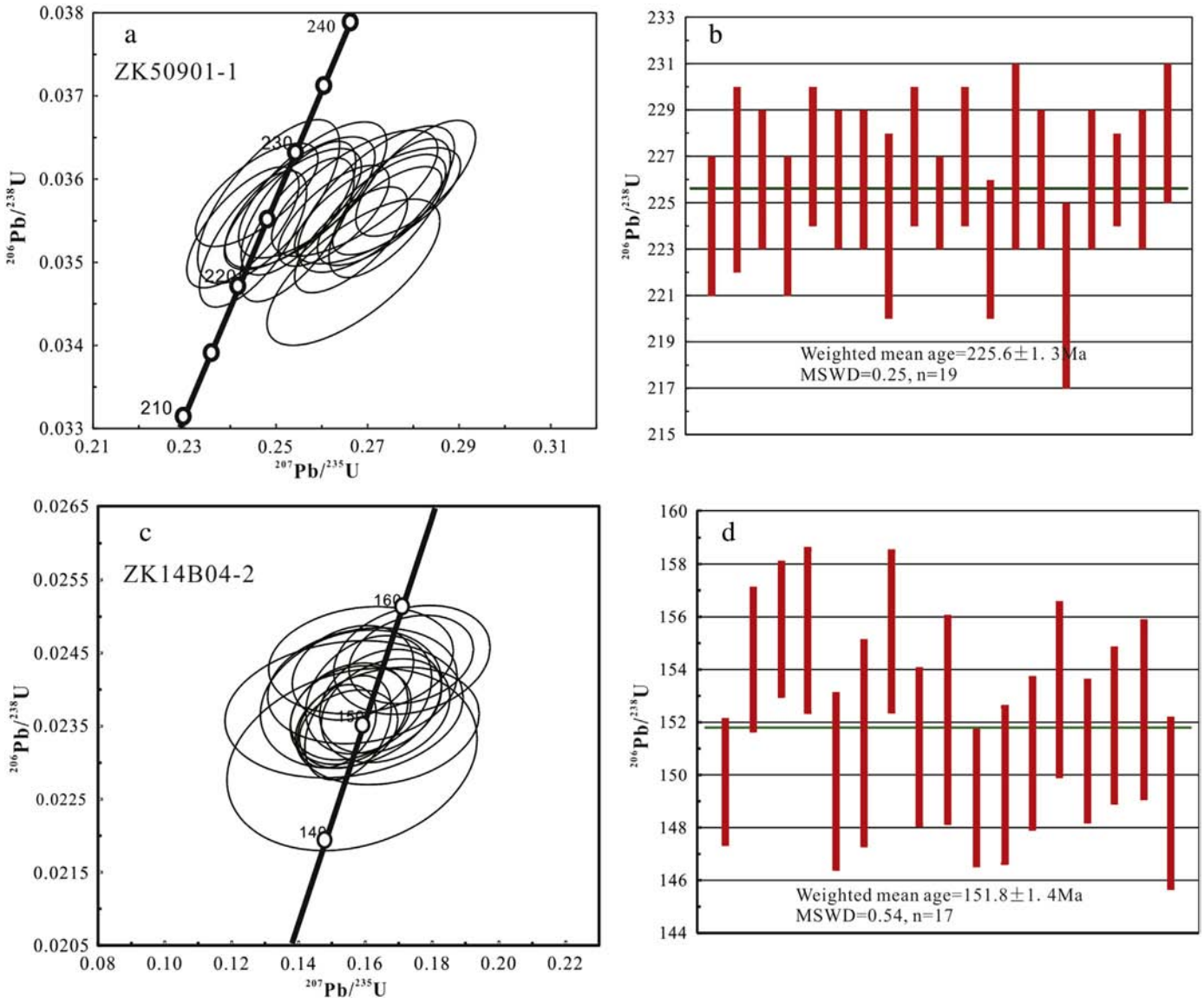

Fig. 6. LA-ICPMS U–Pb concordia age plots (a, c) and weighted average diagrams (b, d) for zircons from the Mesozoic granite of the Xitian deposit. (a, b): the coarse-grained porphyritic K-feldspar granite (ZK50901-1); (c, d): the fine-grained biotite granite (ZK14B04-2).

For sample ZK50901-1, a number of 20 spots were carried out on twenty zircons (Table 1). Only spot ZK50901-1-10 was excluded for its low (<90%) concordance level (Fig. 6a). These spots have a variable abundance of U, 390–5,303 ppm and Th, 103–4,286 ppm, with a Th/U ratio of 0.11–1.84, typical of magmatic zircons (Rubatto, 2002; Corfu et al., 2003). After common lead correction, $^{207}Pb/^{206}Pb$ ages can be used for zircons which are >1.0 Ga in ages, and $^{206}Pb/^{238}U$ ages can be used for younger zircons (Andersen, 2002). The ISOPLOT program (version 3.0; Ludwig, 2003) was used to calculate the $^{206}Pb/^{238}U$ weighted mean age, 225.6 ± 1.3 Ma (n = 19, MSWD = 0.25; Fig. 6b), representing the crystallization age of the coarse-grained porphyritic biotite K-feldspar granite.

For sample ZK14B04-2, seventeen spots were carried out on seventeen different zircons (Table 1). All of them have a large concordance level (Fig. 6c). They have a small abundance range of 162–1,273 ppm for U and 91–480 ppm for Th. The Th/U ratio has a value of 0.27–0.80,

Table 2
Re–Os data for molybdenites from the Xitian W–Sn deposit.

Sample no.	Weight (g)	Re (ppm)		^{187}Re (ppm)		^{187}Os (ppb)		Model ages (Ma)	
		Measured	2σ	Measured	2σ	Measured	2σ	Measured	2σ
ST201016-1	0.1089	8.67401	0.02287	5.4520	0.01437	13.8736	0.1185	150.35	1.36
ST201016-2	0.1023	18.5982	0.0558	11.6897	0.0351	29.5714	0.225	153.56	1.24
ST201016-3	0.0517	41.9488	0.1744	26.3664	0.1096	66.1320	0.5432	150.36	1.59
ST201016-4	0.0528	43.9859	0.2241	27.6469	0.14087	69.1082	0.4677	149.85	0.96
ST201016-5	0.0528	39.1277	0.1214	24.5933	0.0763	61.6665	0.3976	150.32	0.82

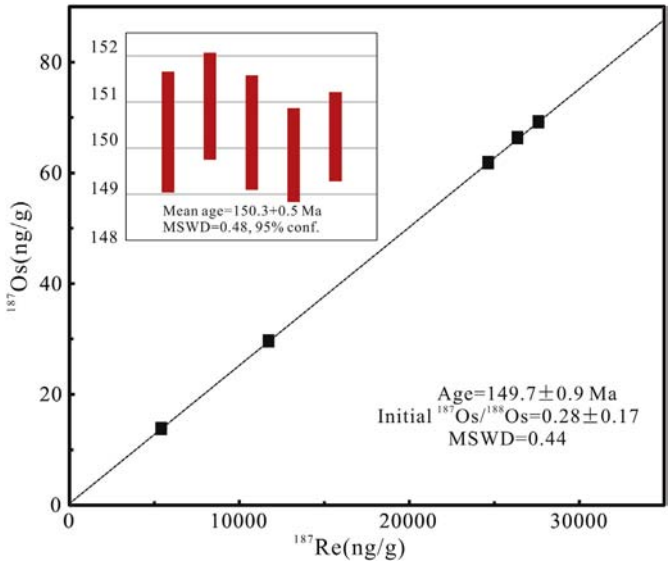

Fig. 7. Re–Os isochron diagram for five molybdenite samples from the Xitian W–Sn deposit.

indicating typical magmatic origin (Rubatto, 2002; Corfu et al., 2003). The $^{206}Pb/^{238}U$ weighted mean age is 151.8 ± 1.4 Ma (n = 17, MSWD = 0.63; Fig. 6d), which is interpreted as the age of crystallization of the fine-grained porphyritic biotite granite.

5.2. Molybdenite Re–Os ages

Listed in Table 2 are the concentrations of Re and Os, and the osmium isotopic compositions of molybdenites for samples ST201016-1 to ST201016-5. Total Re and ^{187}Os contents varied from 8.67 to 43.99 ppm and from 13.87 to 69.11 ppb, respectively. The Re–Os model ages of five molybdenite samples had a relatively narrow range of 149.9 ± 1.0 Ma–150.9 ± 1.2 Ma, and a weighted mean age of 150.3 ± 0.5 Ma with MSWD = 0.48. The ISOPLOT program (Ludwig, 2003) was used to calculate the isochron age, 149.7 ± 0.9 Ma with MSWD = 0.44 (Fig. 7), for these molybdenite grains. Both the model age and the isochron ages are nearly identical, illustrating the reliability of these analytical results.

5.3. Muscovite ^{40}Ar–^{39}Ar ages

As shown in previous studies (Yu and Mao, 2004; Peng et al., 2006), there may be reliable $^{40}Ar/^{39}Ar$ ages for hydrothermal ore deposits under some appropriate conditions. Twelve and fifteen heating steps at temperatures of 450–1,300°C and 450–1,360°C were performed for samples ST201001 and ST201005-1, respectively. The Ar–Ar age spectra of the analyzed samples are presented in Fig. 8, and the results of the Ar–Ar data are summarized in Table 3. Plateau ages were determined using the criteria of Dalrymple and Lanphere (1971). Sample ST201001 has a well-defined plateau age of 149.5 ± 1.5 Ma that encompass 90.08 percent of the gas released, with an isochron age of 149.9 ± 1.5 Ma (Fig. 8; Table 3). Sample ST201005-1 has a similar well-defined plateau age of

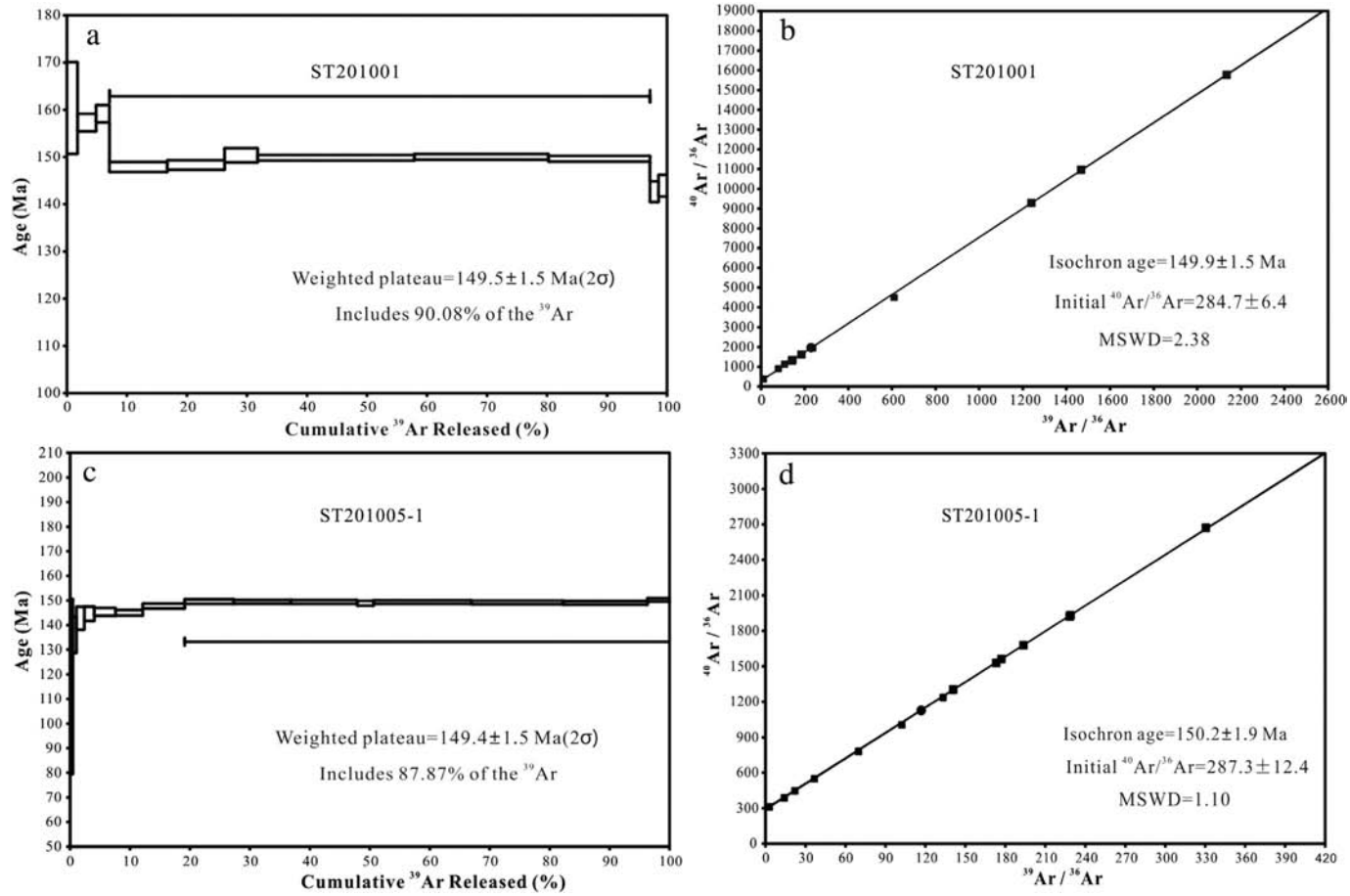

Fig. 8. ^{39}Ar–^{40}Ar age spectra and isochron for two muscovite samples from the Xitian W–Sn deposit.

Table 3
$^{40}Ar/^{39}Ar$ stepwise heating analytical data for two muscovite samples from the Xitian W–Sn deposit, South China.

T(°C)	$^{40}Ar/^{39}Ar$	$^{36}Ar/^{39}Ar$	$^{37}Ar/^{39}Ar$	$^{40}Ar^*/^{39}Ar$ (k)	$^{40}Ar^*$ (%)	$^{39}Ar_k$ (%)	Apparent age (Ma)
ST201001, Sample weight =190.9mg, J=0.0119246							
450	35.4567	0.0936	0.0006	12.4644	21.99	1.76	160.4±9.7
480	11.3758	0.0126	0.0014	21.6744	67.16	3.10	157.3±1.9
510	10.4871	0.0093	0.0004	33.2739	73.76	2.22	159.2±1.8
560	9.2578	0.0071	0.0003	8.0092	77.38	9.66	147.9±1.0
600	8.7838	0.0054	0.0009	8.5955	81.79	9.52	148.3±1.0
700	9.3499	0.0070	0.0014	14.1028	77.96	5.53	150.4±1.5
1150	7.5064	0.0008	0.0001	3.7078	96.74	26.09	149.8±0.6
1210	7.4792	0.0007	0.0006	4.3460	97.23	22.37	150.0±0.6
1240	7.3962	0.0005	0.0010	5.7984	98.05	16.91	149.6±0.6
1270	7.3899	0.0016	0.0326	65.1072	93.36	1.43	142.6±2.2
1300	8.2168	0.0042	0.0269	60.1116	84.75	1.41	143.9±2.3
ST201005-1, Sample weight =207.6mg, J=0.0120724							
450	110.3585	0.35499	0.0002	10.6440	4.94	0.46	115.0±35.6
480	27.4082	0.07076	0.0007	39.7058	23.69	0.60	136.1±7.4
510	20.1723	0.04515	0.0001	26.0574	33.83	1.30	142.8±4.6
550	14.9595	0.02721	0.0001	27.6535	46.22	1.67	144.6±2.9
600	11.1919	0.01432	0.0002	17.4514	62.12	3.56	145.4±1.6
650	9.8305	0.00978	0.0000	15.5476	70.54	4.54	145.0±1.1
700	9.2915	0.0075	0.0001	10.8886	76.08	6.99	147.7±1.0
740	9.2629	0.0071	0.0000	9.4634	77.28	8.17	149.5±0.9
800	8.8289	0.00565	0.0001	8.5123	81.03	9.52	149.4±0.8
860	8.6825	0.00517	0.0001	7.4211	82.35	11.10	149.4±0.8
880	8.8383	0.00577	0.0003	29.6088	80.63	2.72	148.9±1.0
960	8.4472	0.00437	0.0001	5.1877	84.64	16.31	149.4±0.7
1060	8.4390	0.00437	0.0000	5.5210	84.64	15.33	149.2±0.7
1160	8.4334	0.00438	0.0001	6.0091	84.57	14.07	149.0±0.8
1360	8.0941	0.00303	0.0003	24.2732	88.88	3.66	150.2±0.7

149.4 ± 1.5 Ma that contain 80.89 percent of the gas released, with an isochron age of 150.2 ± 1.9 Ma (Fig. 8; Table 3).

6. Discussion

6.1. Re contents and origin of ore metals

The Re–Os isotope system has been recognized as a possible geochemical tool for not only directly dating mineralization but also tracing the source of metals (Stein et al., 1997, 1998; Ruiz and Mathur, 1999; Wang et al., 2011a, 2011b; Li et al., 2007a, 2014b). Comparing Re contents in molybdenite from various types of endogenous Mo deposits in China, Mao et al. (1999) recognized that Re in molybdenite varies in content from hundreds (a mantle source) to tens (a mixed mantle/crust source) to several ppm (a crust source). Similarly, Stein et al. (2001) found out that deposits with the mantle materials (mantle underplating, mantle metasomatism, melting of mafic or ultramafic rocks) have a higher Re content than deposits with a crustal origin. This variation has been confirmed in numerous other deposits (McCandless and Ruiz, 1993; Suzuki et al., 1996; Selby and Creaser, 2004; Zhang et al., 2004; Berzina et al., 2005).

The Re contents in molybdenites from the Xitian W–Sn deposit range from 8.7 ppm to 44.0 ppm, with an average of 30.5 ppm (Table 2). These values fall into the range of tens of ppm Re. Comparing it with Re contents from other W–Sn deposits in the Nanling region (Table 4) indicates that ore metals in the deposit were derived from a mixed mantle/crust provenance. This is supported by high $^3He/^4He$ ratio of 1.15 to 4.43 and $^{40}Ar/^4He$ ratio of 0.55 to 2.62 from fluid inclusions in the Xitian deposit, which is indicative of a crustal–mantle source (Cai et al., 2004, 2005; Yang et al., 2007; Wu et al., 2011).

The Xitian Early Yanshanian granites, which are closely related to W–Sn mineralization, show some typical geochemical signatures of an A-type granite (Ma et al., 2004; Zhou et al., 2013, 2015). These granites are characterized by high SiO_2 (73.44–78.45 wt.%), moderate Al_2O_3 (11.20–13.90 wt.%) and highly variable Na_2O (0.01–4.24 wt.%) contents, as well as low Fe_2O_3 (0.69–2.07 wt.%), MgO (0.003–0.42 wt.%), CaO (0.25–2.22 wt.%), TiO_2 (0.03–0.19 wt.%) and P_2O_5 (0.004–0.04 wt.%) contents. Their ΣREEs have a value of $159–351\times10^{-6}$, $(La/Yb)_N$ 1.35–5.40, and Eu anomalies 0.004–0.08 (Zhou et al., 2015). Their in-situ zircon $\varepsilon_{Hf}(t)$ values range from −4.30 to −14.69, and their $\varepsilon_{Nd}(t)$ values are −9.2 to −7.3, with corresponding T_{DM2} ages of 1.72–1.56 Ga (Yao et al., 2013; Zhou et al., 2015; Su et al., 2015). These characteristics indicate that the early Yanshanian granites have originated from partial melting of metamorphosed rocks in the basement, with some input of a certain amount of mantle-derived materials (Liu et al., 2008a; Yao et al., 2013; Zhou et al., 2013, 2015).

6.2. Ages of magmatism and mineralization

The closure temperature for the Re–Os isotope system in molybdenite is estimated at about 500°C (Suzuki et al., 1996), and is not easily disturbed by post-mineralization hydrothermal, metamorphic and/or tectonic events (Stein et al., 2001). The K–Ar closure temperature for muscovite is less certain but in a range of 350–640°C (Hames and Bowring, 1994). In the Xitian W–Sn deposit, fluid inclusions of quartz

Table 4
Concentrations of Re in W–Sn deposits in the Nanling region.

Deposit	Contents of Re (ppm)	Source of Re	Reference
Dengfuxian quartz vein-type W deposit	0.003–0.098	crust	Cai et al. (2012)
Huangshaping skarn-type Pb–Zn–W–Mo deposit	0.46–25.9	crust	Yao et al. (2007)
Yaogangxian greisen- and skarn-type W–Sn–Bi–Mo–Be deposit	0.1–4.9	crust	Peng et al. (2006)
Maoping greisen-type W–Sn deposit	0.08–0.72	crust	Zeng et al. (2009)
Piaotang quartz vein-type W deposit	0.037–22.3	crust	Zhang et al. (2009)
Zhangtiantang altered granite-type W deposit	0.03–0.079	crust	Feng et al. (2007a)
Hukeng quartz vein-type W deposit	2.85–7.45	crust	Liu et al. (2008b)
Shizhuyuan skarn- and greisen-type W–Sn–Bi–Mo deposit	1.04–1.34	crust	Li et al. (1996)
Da'ao greisen- and vein-type W–Sn deposit	0.029–1.17	crust	Fu et al. (2007)
Hongling quartz vein- or altered granite-type W deposit	1.3–14.57	crust	Wang et al. (2010a)
Shigushan quartz vein-type W–Bi deposit	0.57–1.5	crust	Fu et al. (2008)
Shirenzhang quartz vein-type W deposit	0.48–5.04	crust	Fu et al. (2008)
Zhangdou quartz vein-type W deposit	0.252–0.523	crust	Feng et al. (2011)
Niuling quartz vein-type W–Sn deposit	0.029–13.1	crust	Feng et al. (2011)
Meiziwo quartz vein-type W–Sn deposit	0.72–4.66	crust	Qi et al. (2012)
Yaoling quartz vein-type W–Sn deposit	0.46–3.8	crust	Qi et al. (2012)
Xintianling skarn-type W–Mo deposit	20.56–34.69	crust-mantle mixture	Yuan et al. (2012)
Jinwutang skarn-type Sn–Bi deposit	4.89–30.36	crust-mantle mixture	Liu et al. (2012)
Hehuaping skarn-type Sn deposit	9.29–86.65	crust-mantle mixture	Cai et al. (2006)
Wangshe quartz vein-type W deposit	22.92–32.91	crust-mantle mixture	Lin et al. (2008)
Dabaoshan skarn-type W–Mo polymetallic deposit	64.7–102.4	crust-mantle mixture	Wang et al. (2011b)

and fluorite crystals have three intervals of homogenization temperatures: 290–380°C, 210–240°C and 90–190°C (Yang et al., 2007). These temperatures are much lower than the closure temperatures of the Re–Os molybdenite and Ar–Ar mica chronometers. Thus, the Re–Os and Ar–Ar ages reported in this study are sufficiently reliable to characterize the timing of ore formation in the Xitian W–Sn polymetallic deposit.

Molybdenites in ore-bearing quartz-veins of the Xitian deposit give a Re–Os isochron age of 149.7 ± 0.9 Ma (Fig. 7); these are similar to previous results (Liu et al., 2008a; Guo et al., 2014). These ages are not in agreement with the LA-ICPMS zircon U–Pb age of 225.6 ± 1.3 Ma for the Indosinian K-feldspar granite (Fig. 6a-b) but they do agree with the well-constrained LA-ICPMS zircon U–Pb age of 151.8 ± 1.4 Ma for the Early Yanshanian granite (Fig. 6c-d) and the muscovite $^{40}Ar/^{39}Ar$ isochron ages of 149.9 ± 1.5 Ma and 150.2 ± 1.9 Ma for the greisen samples (Fig. 8). The slight difference between these ages indicates a close relation between the W-Sn mineralization of the Xitian deposit and the Early Yanshanian granitic magmatic event. As a rule of thumb, the Re-Os ages of molybdenites are slightly younger (<6 Ma) than the LA-ICPMS zircon U-Pb ages of ore forming-related intrusions, and are a little older than mica Ar-Ar ages (Selby et al., 2002; Guo, et al., 2011).

Sn, W, Bi, Mo, Cu and Li in the Xitian Early Yanshanian granites have a value of 1.2–43.2 ppm, 25.3–49.7 ppm, 0.4–15.7 ppm, 4.0–18.8 ppm, 36.1–320.4 ppm and 79.0–387.2 ppm, respectively, all being 10 to 20 times than their Clark values, which are 2.2 ppm, 1.1 ppm, 0.025 ppm, 1.1 ppm, 68 ppm, and 17 ppm, respectively (Taylor, 1964), whereas Sn and W in the Indosinian granites have a much lower abundance (Liu et al., 2008a; Fu et al., 2012; Yao et al., 2013). This suggests that the Early Yanshanian granite be more closely tied to the W–Sn mineralization, thus probably providing ore-forming materials for the mineralization (Liu et al., 2008a; Zhou et al., 2015).

According to previous studies of the Xitian granite, the Early Yanshanian granites are characterized by high Si (73.44–78.45 wt.%) and Rb (662–1119 μg/g) contents, low Ti, P, Sr and Ba contents, low

Table 5
U–Pb zircon, Re–Os molybdenite and $^{40}Ar/^{39}Ar$ muscovite/biotite ages from different mineralization styles in the W–Sn deposits of the Nanling region.

Deposit	Mineralization type	Analyzed phase	Age (Ma)	Method	Reference
Hunan Province					
Xitian	skarn- and vein-type W–Sn deposit	zircon in granite	151.8 ± 1.4	LA-ICPMS	This study
		molybdenite	149.7 ± 0.9	Re–Os	This study
		muscovite	149.5 ± 1.5, 149.4 ± 1.5	Ar–Ar	This study
Dengfuxian	quartz vein-type W deposit	molybdenite	150.5 ± 5.2	Re–Os	Cai et al. (2012)
Huangshaping	skarn-type Pb–Zn–W–Mo deposit	zircon in granite	161.6 ± 1.1	LA-ICPMS	Yao et al. (2005)
		molybdenite	154.8 ± 1.9	Re–Os	Yao et al. (2007)
Furong	greisen- and quartz vein-type Sn deposit	zircon in granite	160 ± 2	SHRIMP	Yao et al. (2007)
		biotite	157.5 ± 0.3	Ar–Ar	Mao et al. (2004a)
		muscovite	156 ~ 160	Ar–Ar	Peng et al. (2007)
Yaogangxian	greisen- and skarn-type W–Sn–Bi–Mo–Be deposit	molybdenite muscovite	154.9 ± 2.6	Re–Os	Peng et al. (2006)
			153.0 ± 1.1	Ar–Ar	
Hehuaping	skarn-type Sn deposit	zircon in granite	212 ± 4	SHRIMP	Wei et al. (2007)
		molybdenite	224.0 ± 1.9	Re–Os	Cai et al. (2006)
Xintianling	skarn-type W–Mo deposit	molybdenite	159.1 ± 2.6	Re–Os	Yuan et al. (2012)
Xianghualing	alteration granite- or skarn-type Nb–Ta–W–Sn deposit	Muscovite	154.4 ± 1.1, 161.3 ± 1.1, 158.7 ± 1.2	Ar–Ar	Yuan et al. (2007)
Shizhuyuan	skarn- and greisen-type W–Sn–Bi–Mo deposit	zircon in granite	152 ± 2	SHRIMP	Li et al. (2004)
		molybdenite	151.0 ± 3.5	Re–Os	Li et al. (1996)
		muscovite	153.4 ± 0.2	Ar–Ar	Mao et al. (2004b)
Jinwutang	skarn-type W–Bi deposit	molybdenite	158.8 ± 6.6	Re–Os	Liu et al. (2012)
Da'ao	greisen- and quartz vein-type W–Sn deposit	zircon in granite	156 ± 2, 157 ± 1, 156 ± 2	SHRIMP	Fu et al. (2004b)
		molybdenite	151.3 ± 2.4	Re–Os	Fu et al. (2007)
Jiangxi Province					
Dajishan	albitization granite-type W–Nb–Ta–REE deposit	zircon in granite	151.7 ± 1.6	Dilution	Zhang et al. (2006)
		muscovite	144, 147	Ar–Ar	
Hukeng	quartz vein-type W deposit	molybdenite	150.2 ± 2.2	Re–Os	Liu et al. (2008b)
Piaotang	quartz vein-type W deposit	molybdenite	155.0 ± 2.4	Re–Os	Zhang et al. (2009)
		muscovite	153.6 ± 1.5	Ar–Ar	
		Zircon	153.3 ± 1.9	LA-ICPMS	
Maoping	greisen-type W–Sn deposit	molybdenite	156.8 ± 3.9	Re–Os	Zeng et al. (2009)
Taoxikeng	quartz vein-type W deposit	zircon in granite	158.7 ± 3.9, 157.6 ± 3.5	SHRIMP U–Pb	Guo et al. (2011)
		molybdenite	154.4 ± 3.8	Re–Os	
		muscovite	153.4 ± 1.3, 152.7 ± 1.5	Ar–Ar	
Xihuashan	quartz vein-type W deposit	Zircon in granite	158 ~ 155	LA-ICPMS	Yang et al. (2009b)
Xian'etang	quartz vein-type W deposit	muscovite	231.4 ± 2.4	$^{40}Ar–^{39}Ar$	Liu et al. (2008c)
Muziyuan	quartz vein-type W deposit	molybdenite	155.0 ± 2.4	Re–Os	Zhang et al. (2009)
Niuling	quartz vein-type W–Sn deposit	molybdenite	154.9 ± 4.1	Re–Os	Feng et al. (2007b)
Yaolanzhang	altered granite-type W deposit	molybdenite	155.8 ± 2.8	Re–Os	Feng et al. (2007a)
Guangxi Province					
Huashan–Guposhan	quartz vein-type W deposit	zircon in granite	163 ± 4, 160 ± 4	SHRIMP	Zhu et al. (2005)
		zircon in granite	160.8 ± 1.6, 165 ± 1.9, 163 ± 1.3	LA-ICPMS	Gu et al. (2007)
Liguifu	quartz vein-type W deposit	molybdenite	211.9 ± 6.4	Re–Os	Zou et al. (2009)
Limu	quartz vein-type W deposit	muscovite	214.1 ± 1.9	$^{40}Ar–^{39}Ar$	Yang et al. (2009a)
Guangdong Province					
Shirenzhang	quartz vein-type W deposit	molybdenite	159.1 ± 2.2	Re–Os	Fu et al. (2008)
Shigushan	quartz vein-type W–Bi deposit	molybdenite	154.2 ± 2.7	Re–Os	Fu et al. (2008)
Hongling	quartz vein/altered granite-type deposit	molybdenite	159.1 ± 1.5	Re–Os	Wang et al. (2010a)
Meiziwo	quartz vein-type W deposit	molybdenite	157.7 ± 1.4	Re–Os	Qi et al. (2012)
		muscovite	156.2 ± 1.6	Ar–Ar	Zhai et al. (2010)

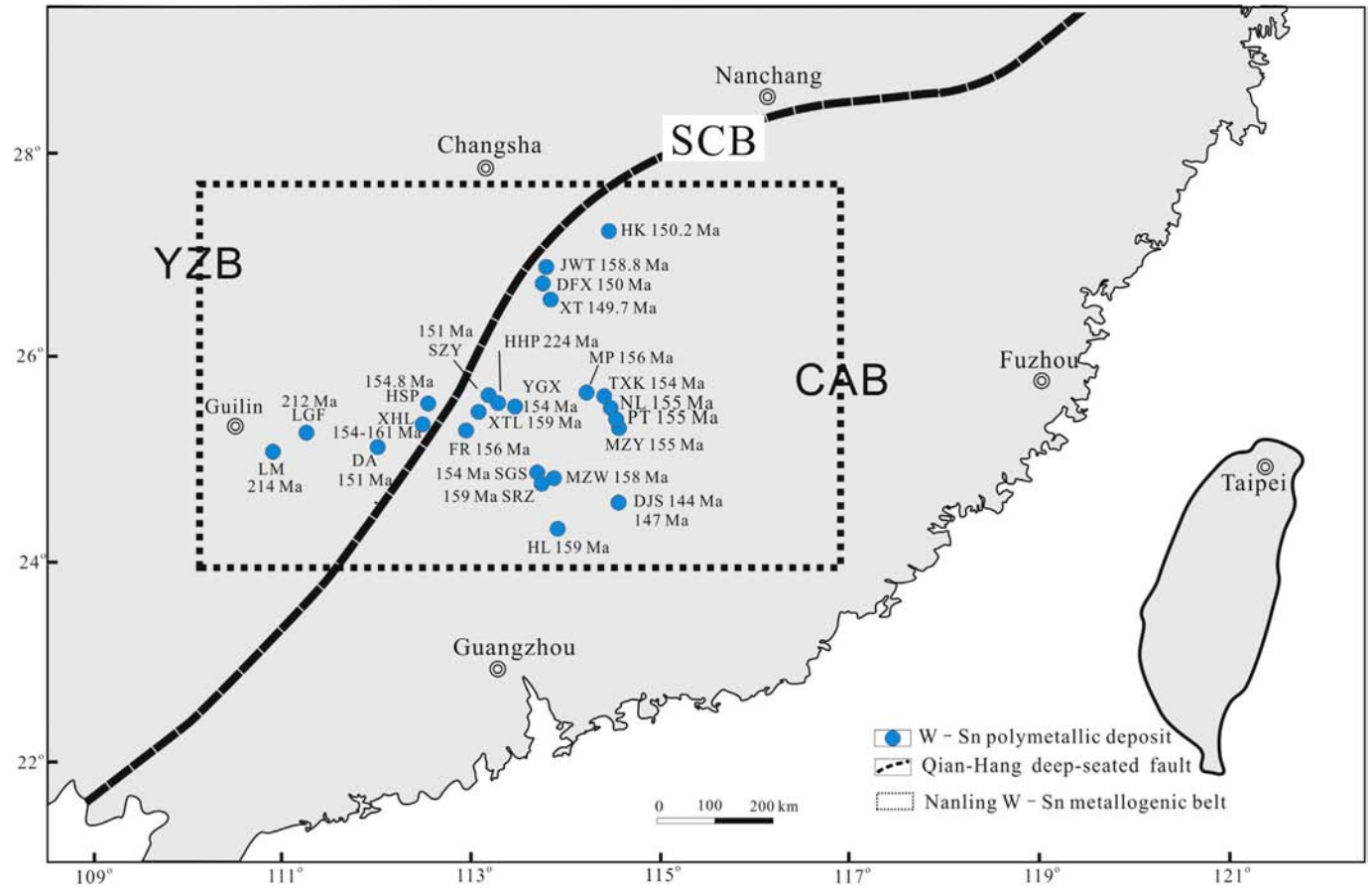

Fig. 9. Distribution of Mesozoic W–Sn deposits and their ages in the Nanling Region (see Table 5 for references). CAB– Cathaysian Block; SCB–South China Block; YZB–Yangtze Block; Deposits: DA-Da'ao; DJS-Dajishan; FR-Furong; HL- Hongling; HK-Hukeng; HL-Hongling; HSP-Huangshaping; JWT-Jinwutang; LGF-Liguifu; LM-Limu; MP-Maoping; MZW-Meiziwo; MZY-Muziyuan; NL-Niuling; PT-Piaotang; SGS-Shigushan; SRZ-Shirenzhang; SZY-Shizhuyuan; TXK-Taoxikeng; XHL-Xianghualing; XT-Xitian; TL-Xintianling; YGX-Yaogangxian.

Rb/Sr and Nb/Ta ratios, and REE patterns with the pronounced tetrad effect (Liu et al., 2008a; Zhou et al., 2015). These features suggest the presence of intense fluid-magma interaction, extremely favorable to W–Sn mineralization (Lehmann and Harmanto, 1990; Jahn et al., 2001; Bastos Neto et al., 2009). In contrast to the Early Yanshanian granites, the Indosinian granites are intermediate to acidic, and have higher Ti,

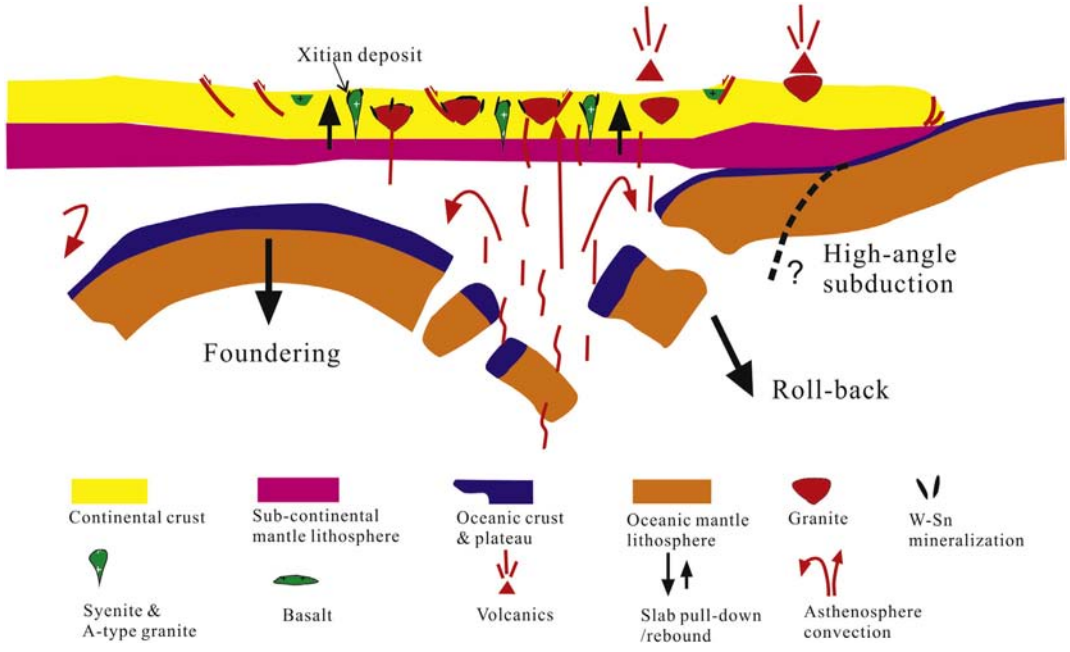

Fig. 10. Schematic diagram showing the Mid- and Late-Jurassic tectonomagmtic evolution and metallogeny of South China. Modified after Li and Li (2007).

P, Sr and Ba contents, but lower Si, Rb and Nb/Ta values, and right-inclined REE patterns (Ma et al., 2004; Yao et al., 2013).

The Jurassic period is an important time interval of granitic magmatism and W–Sn metallogenesis in the Nanling region, South China (Table 5; Fig. 9). Hua et al. (2005) recognized three major metallogenic events in this region in the Mesozoic: Cu–Pb–Zn–(Au) mineralization in 180–170 Ma, W–Sn–Nb–Ta mineralization in 150–139 Ma, and Sn–U mineralization in 125–98 Ma. This last event corresponds with Au–Cu–Pb–Zn–Ag mineralization in the Southeast coastal belt (Pirajno and Bagas, 2002). This does not differ greatly from Mao et al.'s (2007) two stages of W–Sn mineralization in the region: Late Jurassic–Early Cretaceous or 165–150 Ma, and Mid-Cretaceous or 130–90 Ma. A recently increasing number of isotopic datings define an accurately narrow age interval of 165–145 Ma, for a majority of W–Sn deposits there, which are in correspondence with intense Late Jurassic magmatic activity (Table 5) (Li et al., 1996, 2014a; Peng et al., 2006; Fu et al., 2007, 2008; Feng et al., 2007a, 2007b; Tan et al., 2007; Yao et al., 2007; Yuan et al., 2007, 2012; Liu et al., 2008b, 2012; Yang et al., 2009a, 2009b; Zhang et al., 2009; Zou et al., 2009; Wang et al., 2010a; Zhai et al., 2010; Guo et al., 2011; Qi et al., 2012). The close relationship between the Xitian deposit and the Early Yanshanian granites, as discussed in the previous subsection, is a good example of this relationship.

6.3. Geodynamics for W–Sn metallogeny

Widespread, intense Yanshanian granitic magmatism and mineralization in South China have attracted attention of geologists (Jahn et al., 1976; Charvet et al., 1994; Lan et al., 1996; Sewell and Campbell, 1997; Wang et al., 2010b, 2011a, 2011b). However, the tectonic regime responsible for the Yanshanian magmatism and related W–Sn mineralization is still debated. Gilder et al. (1996) identified the NNE-trending Shi–Hang granite belt, characterized by low T_{DM} (neodymium depleted mantle model age) values and relatively high ε_{Nd} values in central South China, and attributed it to the coeval processes of lithospheric extension and crust–mantle interaction. Mao et al. (1998) proposed the mantle plume model to explain the extensive polymetallic mineralization and associated granites in the Mesozoic of South China. Zhou and Li (2000) emphasized the importance of a gradual change in dip angle of the westward subducting Paleo-Pacific plate beneath the SCB in 180–80 Ma. Hua et al. (2005) believed the mantle upwelling, as a result of lithospheric thinning and crustal extension, led to copious granitoids and associated W–Sn polymetallic mineralization in the SCB during the Yanshanian. Li and Li (2007) proposed the flat-slab subduction and slab-foundering model to account for both the widespread Indosinian orogeny and the widespread Mesozoic magmatism in South China.

Rapidly growing geochronological data in the Nanling region have revealed the close relation of most W–Sn polymetallic deposits to granites of 165–150 Ma in age (Fig. 9; Table 5; Peng et al., 2006, 2008; Yao et al., 2007; Fu et al., 2007, 2008; Feng et al., 2007a, 2007b; Yuan et al., 2007, 2012; Liu et al., 2008b, 2012; Yang et al., 2009a, 2009b; Zhang et al., 2009; Zou et al., 2009; Wang et al., 2010a; Zhai et al., 2010; Guo et al., 2011; Qi et al., 2012; Li et al., 2014a). In the Xitian area, the Early Yanshanian granites, genetically related to W–Sn mineralization, are identified as A_2- type (Zhou et al., 2013, 2015). A-type granites are generally considered to form in various extensional tectonic settings, such as back-arc, post-collisional extension or continental interior, regardless of the origin of the magma source (e.g. Whalen et al., 1987; Eby, 1992; Turner et al., 1992). In this sense, we would like to attribute the Early Yanshanian granites of A_2-type to back-arc extension (Zhou et al., 2013, 2015; Mao et al., 2013a) rather than the mantle plume or the continental rifting (Mao et al., 1998), based on the following regional geological data:

(1) The NNE-trending Shi-Hang (from Shiwandashan in the west to Hangzhou in the east) high-ε_{Nd} granite belt in the interior of South China (Gilder et al., 1996; Hong et al., 2002; Mao et al., 2013a; Zhou et al., 2015), where the Xitian deposit lies, is probably a Neoproterozoic suture zone between the YZB and CAB. The flat subduction of the Paleo-Pacific plate beneath the SCB in Mesozoic might have terminated beneath the belt, where there existed contemporaneous bimodal magmatism, diagnostic of the continental arc to intra-arc rift setting due to slab rollback (Jiang et al., 2009 and references therein);

(2) The Early Yanshanian granitic magmatism took place only in the Nanling region, with a southeastward-younging trend, in comparison with the distribution of the Late Yanshanian (140–90 Ma) volcanic and intrusive rocks near to the coast (Gilder et al., 1991; Chen and Jahn, 1998; Zhou and Li, 2000; Sun et al., 2003; Wang et al., 2005; Li et al., 2006; Li and Li, 2007; Li et al., 2007a).

Li and Li (2007) attributed this younging trend to the slab rollback or high-angle subduction of the Paleo-Pacific plate (Fig. 10). Foundering of the flab-slab likely occurred during Middle Jurassic, and resulted in strong upwelling of the asthenosphere mantle, mafic underplating, and extensive mantle-crust interaction. These deep processes increased the geothermal flow, which eventually induced widespread emplacement of I-type or A-type granites and their related W–Sn polymetallic mineralization throughout the Nanling and adjacent areas during 160–150 Ma (Mao et al., 2007, 2008, 2013a).

7. Conclusions

Dating of the Xitian W–Sn polymetallic deposit in eastern Hunan Province using Re–Os molybdenite, Ar–Ar muscovite and LA-ICPMS U–Pb zircon techniques enables us to draw the following conclusions:

1) Molybdenites in ore-bearing quartz veins of the Xitian deposit are characterized by a relatively variable Re content, 8.7–44.0 ppm, with an average of 30.5 ppm, indicating that the ore-forming materials were derived from the mixed mantle and crustal sources.

2) LA-ICPMS zircon U–Pb dating yields a crystallization age of 225.6 ± 1.3 Ma for the Indosinian granites, in no relation to W–Sn mineralization. Molybdenites have a Re–Os age of 149.7 ± 0.9 Ma, slightly smaller than the LA-ICPMS zircon U–Pb age of the Yanshanian granites, 151.8 ± 1.4 Ma, and similar to two muscovite $^{40}Ar/^{39}Ar$ ages of ore-bearing greisen, 149.5 ± 1.5 Ma and 149.4 ± 1.5 Ma. That is to say, W–Sn mineralization took place immediately after the emplacement of the Early Yanshanian granites.

3) These data are generally consistent with previously published isotopic ages, also indicative of large-scale W–Sn polymetallic mineralization in late Jurassic or 160–150 Ma in the Nanling region. This regional mineralization is interpreted as in the back-arc extensional setting, which was probably triggered by the break-off or foundering of the subducted flat-slab beneath the lithosphere.

Acknowledgements

This work was financially supported by the Public Scientific Research Project of Ministry of Land and Resources of China (201211024-03) and National Natural Science Foundation of China (Nos. 41576040, 40872080 & 41072081). The authors are indebted to Y. L. Sun, Y. Liu and G. Q. Hu for their help with sample analysis. Dr Susan Turner and two reviewers (Prof. J. W. Mao, and Dr. C.L. Guo) are thanked for science and English language improvements of the original and revised manuscripts. Special thanks are due to the Associate Editor (Dr. Lightfoot) for assisting us in editing this manuscript.

References

Andersen, T., 2002. Correction of common lead in U–Pb analyses that do not report ^{204}Pb. Chem. Geol. 192, 59–79.

Bai, D., Chen, J.C., Ma, T.Q., Wang, X.H., 2005. Geochemical characteristics and tectonic setting of Qitianling A-type granitic pluton in southeast Hunan. Acta Petrol. Mineral. 24, 255–272 (in Chinese with English abstract).

Bastos Neto, A.C., Pereira, V.P., Ronchi, L.H., DeLima, E.F., Frantz, J.C., 2009. The world-class Sn, Nb, Ta, F (Y, REE, Li) deposit and the massive cryolite associated with the albite-enriched facies of the Madeira A-type granite, Pitinga mining district, Amazonas state, Brazil. Can. Mineral. 47, 1329–1357.

Berzina, A.N., Sotnikov, V.I., Economou-Eliopoulos, M., Eliopoulos, D.G., 2005. Distribution of rhenium in molybdenite from porphyry Cu–Mo and Mo–Cu deposits of Russia (Siberia) and Mongolia. Ore Geol. Rev. 26, 91–113.

Black, L.P., Kamo, S.L., Allen, C.M., Aleinikoff, J.N., Davis, D.W., Korsch, R.J., Foudoulis, C., 2003. TEMORA 1: a new zircon standard for Phanerozoic U–Pb geochronology. Chem. Geol. 200, 155–170.

Cai, X.H., Jia, B.H., 2006. Discovery of the Xitian tin deposit, Hunan, and its ore potential. Geol. China 33, 1100–1108 (in Chinese with English abstract).

Cai, M.H., Mao, J.W., Liang, T., Wu, F.X., 2004. Helium and argon isotopic component s of f luid inclusions in Dachang tin-polymetallic deposit and their geological implications. Mineral Deposits 23, 225–231 (in Chinese with English abstract).

Cai, M.H., Mao, J.W., Liang, T., Huang, H.L., 2005. Fluid inclusion studies of Tongkeng-Changpo deposit in Dachang polymetallic tin oref ield. Mineral Deposits 24, 228–241 (in Chinese with English abstract).

Cai, M.H., Chen, K.X., Qu, W.J., Liu, G.Q., Fu, J.M., Yin, J.P., 2006. Geological characteristics and Re–Os dating of molybdenites in Hehuaping tin-polymetallic deposit, southern Hunan Province. Mineral Deposits 25, 263–269 (in Chinese with English abstract).

Cai, Y., Ma, D.S., Lu, J.J., Huang, H., Zhang, R.Q., Qu, W.J., 2012. Re–Os geochronology and S isotope geochemistry of Dengfuxian tungsten deposit, Hunan Province, China. Acta Petrol. Sin. 28, 3798–3808 (in Chinese with English abstract).

Charvet, J., 2013. The Neoproterozoic–Early Paleozoic tectonic evolution of the South China Block: An overview. J. Asian Earth Sci. 74, 198–209.

Charvet, J., Lapierre, H., Yu, Y.W., 1994. Geodynamic significance of the Mesozoic volcanism of southeastern China. J. Southeast Asian Earth Sci. 9, 387–396.

Che, Q., Li, J., Wei, S., 2005. Elementary Discussion of the Tectonic Background of Deposit–Concentrated Qianlishan–Qitianling Area in Hunan. Geotecton. Metallog. 29, 204–214 (in Chinese with English abstract).

Chen, J.F., Jahn, B.M., 1998. Crustal evolution of southeastern China: Nd and Sr isotopic evidence. Tectonophysics 284, 101–133.

Chen, D., Ma, A.J., Liu, W., Liu, Y.R., Ni, Y.J., 2013. Research on U–Pb Chronology in Xitian Pluton of Hunan Province. Geoscience 4, 819–830 (in Chinese with English abstract).

Chen, D., Shao, Y.J., Liu, W., Ma, A.J., Liu, Y.R., 2014. Petrological characteristics of Xitian pluton in Hunan provinve. Geol. Miner. Resour. South China 31, 11–25 (in Chinese with English abstract).

Corfu, F., Hanchar, J.M., Hoskin, P.W.O., Kinny, P.D., 2003. Atlas of Zircon Textures. Rev. Mineral. Geochem. 53, 469–500.

Dalrymple, B.G., Lanphere, M.A., 1971. $^{40}Ar/^{39}Ar$ technique of K–Ar dating: a comparison with the conventional technique. Earth Planet. Sci. Lett. 12, 300–308.

Deng, X.W., Liu, J.X., Dai, X.L., 2015. Geological characteristics and molybdenite Re-Os isotopic age of Hejiangkou tungsten and tin polymetallic deposit,East Hunan, China. Chin. J. Nonferrous Met. 25, 2883–2897 (in Chinese with English abstract).

Du, A.D., Wu, S.Q., Sun, D.Z., Wang, S.X., Qu, W.J., Markey, R., Stain, H., Morgan, J., Malinovskiy, D., 2004. Preparation and Certification certification of Re–Os Dating dating Reference reference Materialsmaterials: Molybdenites molybdenites HLP and JDC. Geostand. Geoanal. Res. 28, 41–52.

Eby, G.N., 1992. Chemical subdivision of the A-type granitoids: petrogenetic and tectonic implications. Geology 20, 641–644.

Feng, C.Y., Feng, Y.D., Xu, J.X., Zeng, Z.L., She, H.Q., Zhang, D.Q., Qu, W.J., Du, A.D., 2007a. Isotope chronological evidence for Upper Jurassic petrogenesis and mineralization of altered granite-type tungsten deposits in the Zhangtiantang area, southern Jiangxi. Geol. China 4, 642–650 (in Chinese with English abstract).

Feng, C.Y., Xu, J.X., Zeng, Z.L., Zhang, D.Q., Qu, W.J., She, H.Q., Li, J.W., Li, D.X., Du, A.D., Dong, Y.J., 2007b. Zircon SHRIMP U—Pb and molybdenite Re–Os dating in Tianmenshan–Hongtaoling tungsten–tin Orefield, Southern Jiangxi Province, China, and its geological implication. Acta Geol. Sin. 81, 952–963.

Feng, C.Y., Zeng, Z.L., Zhang, D.Q., Qu, W.J., Du, A.D., Li, D.X., She, H.Q., 2011. SHRIMP zircon U–Pb and molybdenite Re–Os isotopic dating of the tungsten deposits in the Tianmenshan–Hongtaoling W–Sn orefield, southern Jiangix Province, China, and geological implications. Ore Geol. Rev. 43, 8–25.

Fu, J.M., Ma, C.Q., Xie, C.F., Zhang, Y.M., Peng, S.B., 2004a. Geochemistry and tectonic setting of Xishan aluminous A-type granitic volcanic–intrusive complex, Southern Hunan. J. Earth Sci. Environ. 26, 15–23 (in Chinese with English abstract).

Fu, J.M., Ma, C.Q., Xie, C.F., Zhang, Y.M., Peng, S.B., 2004b. SHRIMP U–Pb zircon dating of the Jiuyishan composite granite in Hunan and its geological significance. Geotecton. Metallog. 28, 370–378 (in Chinese with English abstract).

Fu, J.M., Li, H.Q., Qu, W.J., Yang, X.J., Wei, J.Q., Liu, G.Q., Ma, L.Y., 2007. Re–Os isotope dating of the Da'ao tungsten–tin deposit in the Jiuyi Mountains, southern Hunan Province. Geol. China 4, 651–656 (in Chinese with English abstract).

Fu, J.M., Li, H.Q., Qu, W.J., Ma, L.Y., Yang, X.J., Wei, J.Q., Liu, G.Q., 2008. Determination of mineralization epoch of quartz-vein type tungsten deposit in Shixing region, Northern Guangdong and its significance. Geotecton. Metallog. 32, 57–62 (in Chinese with English abstract).

Fu, J.M., Wu, S.C., Xu, D.M., Ma, L.Y., Cheng, S.B., Chen, X.Q., 2009. Reconstraint from zircon SHRIMP U–Pb dating on the age of magma intrusion and mineralization in Xitian tungsten–tin polymetallic orefield, eastern Hunan Province. Geol. Miner. Resour. South China 37, 1–7 (in Chinese with English abstract).

Fu, J.M., Cheng, S.B., Lu, Y.Y., Wu, S.C., Ma, L.Y., Chen, X.Q., 2012. Geochronology of the greisen-quartz-vein type tungsten–tin deposit and its host granite in Xitian, Hunan Province. Geol. Explor. 48, 313–320 (in Chinese with English abstract).

Gao, S., Ling, W.L., Qiu, Y.M., Lian, Z., Hartmann, G., Simon, K., 1999. Contrasting geochemical and Sm–Nd isotopic compositions of Archean metasediments from the Kongling high-grade terrain of the Yangtze craton: evidence for cratonic evolution and redistribution of REE during crustal anatexis. Geochim. Cosmochim. Acta 63, 2071–2088.

Gao, S., Liu, X., Yuan, H., Hattendorf, B., Günther, D., Chen, L., Hu, S., 2002. Determination of Forty Two Major and Trace Elements in USGS and NIST SRM Glasses by Laser Ablation-Inductively Coupled Plasma-Mass Spectrometry. Geostand. Newslett. 26, 181–196.

Gilder, S.A., Keller, G.R., Luo, M., Goodell, P.C., 1991. Timing and spatial–distribution of rifting in China. Tectonophysics 197, 225–243.

Gilder, S.A., Gill, J., Coe, R.S., Zhao, X.X., Liu, Z.W., Wang, G.X., Yuan, K.R., Kuang, G.D., Wu, H.R., 1996. Isotopic and paleomagnetic constraints on the Mesozoic tectonic evolution of south China. J. Geophys. Res. 101, 16137–16154.

Gu, S.Y., Hua, R.M., Qi, H.W., 2007. Zircon LA-ICPMS U-Pb dating and Sr–Nd isotope study of the Guposhan granite complex, Guangxi, China. Chin. J. Geochem. 26, 290–300.

Guo, C.L., Mao, J.W., Bierlein, F., Chen, Z.H., Chen, Y.C., Li, C.B., Zeng, Z.L., 2011. SHRIMP U–Pb (zircon), Ar–Ar (muscovite) and Re–Os (molybdenite) isotopic dating of the Taoxikeng tungsten deposit, South China Block. Ore Geol. Rev. 43, 26–39.

Guo, C.L., Li, C., Wu, S.C., Xu, Y.M., 2014. Molybdenite Re–Os Isotopic Dating of Xitian Deposit in Hunan Province and Its Geological Significance. Rock Miner. Anal. 33, 142–152 (in Chinese with English abstract).

Hames, W.E., Bowring, S.A., 1994. An empirical evaluation of the argon diffusion geometry in muscovite. Earth Planet. Sci. Lett. 124, 161–169.

HNBGMR (Hunan Bureau of Geology and Mineral Resources), 1988. Regional Geology of the Hunan Province. Geological Publishing House, Beijing (507 pp.).

Hong, D.W., Xie, X.L., Zhang, J.S., 2002. Geological significance of the Hangzhou–Zhuguangshan–Huashan high–ε_{Nd} granite belt. Geol. Bull. China 21, 348–354.

Hsü, K.C., 1943. Tungsten deposits of southern Kiangsi, China. Econ. Geol. 38, 431–474.

Hu, R.Z., Bi, X.W., Jiang, G.H., Chen, H.W., Peng, J.T., Qi, Y.Q., Wu, L.Y., Wei, W.F., 2012a. Mantle-derived noble gases in ore-forming fluids of the granite-related Yaogangxian tungsten deposit, Southeastern China. Mineral. Deposita 47, 623–632.

Hu, R.Z., Wei, W.F., Bi, X.W., Peng, J.T., Qi, Y.Q., Wu, L.Y., Chen, Y.W., 2012b. Molybdenite Re–Os and muscovite $^{40}Ar/^{39}Ar$ dating of the Xihuashan tungsten deposit, central Nanling district, South China. Lithos 150, 111–118.

Hua, R.M., Chen, P.R., Zhang, W.L., Yao, J.M., Lin, J.F., Zhang, Z.S., Gu, S.Y., Liu, X.D., Qi, H.W., 2005. Metallogenesis related to Mesozoic Granitoids in the Nanling Range, South China and their geodynamic settings. Acta Geol. Sin. 79, 810–820.

Huang, H.Q., Li, X.H., Li, W.X., Li, Z.X., 2011. Formation of high $\delta^{18}O$ fayalite-bearing A-type granite by hightemperature melting of granulitic metasedimentary rocks, southern China. Geology 39, 903–906.

Jahn, B.M., Chen, P.Y., Yen, T.P., 1976. Rb–Sr ages of granitic rocks in southeastern China and their tectonic significance. Geol. Soc. Am. Bull. 87, 763–776.

Jahn, B.M., Wu, F.Y., Capdevila, R., Martineau, F., Zhao, Z.H., Wang, Y.X., 2001. Highly evolved juvenile granites with tetrad REE patterns: the Woduhe and Baerzhe granites from the Great Xing'an Mountains in NE China. Lithos 59, 171–198.

Jiang, Y.H., Ling, H.F., Jiang, S.Y., Fan, H.H., Shen, W.Z., Ni, P., 2005. Petrogenesis of a Late Jurassic peraluminous volcanic complex and its high–Mg, potassic, quenched enclaves at Xiangshan, southeast China. J. Petrol. 46, 1121–1154.

Jiang, Y.H., Jiang, S.Y., Zhao, K.D., Ling, H.F., 2006. Petrogenesis of Late Jurassic Qianlishan granites and mafic dykes, Southeast China: implications for a backarc extension setting. Geol. Mag. 143, 457–474.

Jiang, Y.H., Jiang, S.Y., Dai, B.Z., Liao, S.Y., Zhao, K.D., Ling, H.F., 2009. Middle to Late Jurassic felsic and mafic magmatism in southern Hunan province, southeast China: implications for a continental arc to rifting. Lithos 107, 185–204.

Jiang, Y.H., Zhao, P., Zhou, Q., Liao, S.Y., Jin, G.D., 2011. Petrogenesis and tectonic implications of Early Cretaceous S- and A-type granites in the northwest of the Gan–Hang rift, SE China. Lithos 121, 55–73.

Koppers, A.A., 2002. ArArCALC–software for $^{40}Ar/^{39}Ar$ age calculations. Comput. Geosci. 28, 605–619.

Lan, C.Y., Jahn, B.M., Mertzman, S.A., Wu, T.W., 1996. Subduction-related granitic rocks of Taiwan. J. SE Asian Earth Sci. 14, 11–28.

Lehmann, B., Harmanto, 1990. Large-scale tin depletion in the Tanjungpandan tin granite, Belitung Island, Indonesia. Econ. Geol. 85, 99–111.

Li, X.H., 1991. Geochronology of Wanyangshan–Zhuguangshan granitoid batholith: implication for the crust development. Sci. China B 34, 620–629.

Li, X.H., 1998a. The SHRIMP U–Pb zircon geochronology of Paleoproterozoic plagioclase–amphibolite in the Zhejiang–Fujian area. J. Geochem. 27, 327–334.

Li, Z.X., 1998b. Tectonic history of the major East Asian lithospheric blocks since the mid-Proterozoic: a synthesis. In: Flower, M.F.J., Chung, S.L., Lo, C.H., Lee, C.Y. (Eds.), Mantle dynamics and plate interactions in East Asia. American Geophysical Union (Geodynamic series) 27, pp. 221–243.

Li, X.H., 2000. Cretaceous magmatism and lithospheric extension in Southeast China. J. Asian Earth Sci. 18, 293–305.

Li, Z.X., Li, X.H., 2007. Formation of the 1300-km-wide intracontinental orogen and postorogenic magmatic province in Mesozoic South China: A flat–slab subduction model. Geology 35, 179–182.

Li, H.Y., Mao, J.W., Sun, Y.L., Zou, X.Q., He, H.L., Du, A.D., 1996. Re–Os isotopic chronology of molybdenites in the Shizhuyuan polymetallic tungsten deposit, Southern Hunan. Geol. Rev. 42, 261–267 (in Chinese with English abstract).

Li, X.H., Hu, R.Z., Rao, B., 1997. Geochronology and geochemistry of Cretaceous mafic rocks from northern Guangdong Province, SE China. Geochimica 26, 14–31 (in Chinese with English abstract).

Li, X.H., Liu, D.Y., Sun, M., Li, W.X., Liang, X.R., Liu, Y., 2004. Precise Sm–Nd and U–Pb isotopic dating of the supergiant Shizhuyuan polymetallic deposit and its host granite, SE China. Geol. Mag. 141, 225–231.

Li, X.H., Li, Z.X., Li, W.X., Wang, Y.J., 2006. Initiation of the Indosinian Orogeny in South China: evidence for a Permian magmatic arc on Hainan Island. J. Geol. 114, 341–353.
Li, H., Ye, H., Mao, J., Wang, D., Chen, Y., Qu, W., Du, A., 2007a. Re–Os dating of molybdenites from Au (–Mo) deposits in Xiaoqinling gold ore district and its geological significance. Mineral Deposits 26, 417–424 (in Chinese with English abstract).
Li, X.H., Li, W.X., Li, Z.X., 2007b. On the genetic classification and tectonic implications of the Early Yanshanian granitoids in the Nanling Range, South China. Chin. Sci. Bull. 52, 1873–1885.
Li, X.H., Li, Z.X., Li, W.X., Liu, Y., Yuan, C., Wei, G., Qi, C., 2007c. U–Pb zircon, geochemical and Sr–Nd–Hf isotopic constraints on age and origin of Jurassic I– and A–type granites from central Guangdong, SE China: A major igneous event in response to foundering of a subducted flat–slab? Lithos 96, 186–204.
Li, X.H., Watanabe, Y., Mao, J., Liu, S., Yi, X., 2007d. Sensitive High–Resolution Ion Microprobe U–Pb Zircon and ^{40}Ar–^{39}Ar Muscovite Ages of the Yinshan Deposit in the Northeast Jiangxi Province, South China. Resour. Geol. 57, 325–337.
Li, Z.L., Hu, R.Z., Yang, J.S., Peng, J.S., Li, X.M., Bi, X.W., 2007e. He, Pb and S isotopic constraints on the relationship between the A-type Qitianling granite and the Furong tin deposit, Hunan Province, China. Lithos 97, 161–173.
Li, X.H., Li, Z.X., He, B., Li, W.X., Li, Q.L., Gao, Y.Y., Wang, X.C., 2012. The Early Permian active continental margin and crustal growth of the Cathaysia Block: In situ U–Pb, Lu–Hf and O isotope analyses of detrital zircons. Chem. Geol. 328, 195–207.
Li, H., Watanabe, K., Yonezu, K., 2014a. Geochemistry of A-type granites in the Huangshaping polymetallic deposit (South Hunan, China): Implications for granite evolution and associated mineralization. J. Asian Earth Sci. 88, 149–167.
Li, J., Huang, X.L., He, P.L., Li, W.X., Yu, Y., Chen, L.L., 2014b. In situ analyses of micas in the Yashan granite, South China: Constraints on magmatic and hydrothermal evolutions of W and Ta–Nb bearing granites. Ore Geol. Rev. 65, 793–810.
Liang, J.L., Ding, X., Sun, X.M., Zhang, Z.M., Zhang, H., Sun, W.D., 2009. Nb/Ta fractionation observed in eclogites from the Chinese Continental Scientific Drilling Project. Chem. Geol. 268, 27–40.
Lin, Y.Z., Wang, D.H., Li, S.R., 2008. Re–Os isotopic age of molybdenite from the Wangshe copper–tungsten deposit in Guangxi province and their implications. Acta Geol. Sin. 82, 1565–1571 (in Chinese with English abstract).
Liu, G.Q., Wu, S.C., Du, A.D., Fu, J.M., Yang, X.J., Tang, Z.H., Wei, J.Q., 2008a. Metallogenic ages of the Xitian tungsten–tin deposit, Eastern Hunan province. Geotecton. Metallog. 32, 63–71 (in Chinese with English abstract).
Liu, J., Ye, H.S., Xie, G.Q., Yang, G.Q., Zhang, W., 2008b. Re–Os dating of molybdenite from the Hukeng tungsten deposit in the Wugongshan area, Jiangxi Province, and its geological implications. Acta Geol. Sin. 82, 1572–1579 (in Chinese with English abstract).
Liu, S.B., Wang, D.H., Chen, Y.C., Li, J.K., Ying, L.J., Xu, J.X., Zeng, Z.L., 2008c. $^{40}Ar/^{39}Ar$ ages of muscovite from different types tungsten-bearing quartz veins in the Chongyi-Dayu-Shangyou concentrated mineral area in Gannan region and its geological significance. Acta Geol. Sin. 82, 932–940 (in Chinese with English abstract).
Liu, Y.S., Hu, Z.C., Zong, K.Q., Gao, C.G., Gao, S., Xu, J., Chen, H.H., 2010. Reappraisement and refinement of zircon U–Pb isotope and trace element analyses by LA-ICPMS. Chin. Sci. Bull. 55, 1535–1546 (in Chinese).
Liu, X.F., Yuan, S.D., Wu, S.H., 2012. Re–Os dating of the molybdenite from the Jinchuantang tin–bismuth deposit in Hunan Province and its geological significance. Acta Petrol. Sin. 28, 39–51 (in Chinese with English abstract).
Lu, H.Z., 1986. The Origin of Tungsten Mineral Deposits in South China. Chongqing Publishing House, Chongqing (232 pp. (in Chinese with English abstract)).
Lu, H.Z., Liu, Y., Wang, C., Xu, Y., Li, H., 2003. Mineralisation and fluid inclusion study of the Shizhuyuan W–Sn–Bi–Mo–F skarn deposit, Hunan Province, China. Econ. Geol. 98, 955–974.
Ludwig, K.R., 2003. User's Manual for Isoplot/Ex. 3.00: A Geochronological Toolkit for Microsoft Excel. Berkeley Geochronology Center Special Publication, Berkeley, pp. 1–70.
Luo, H.W., Zeng, Q.W., Zeng, G.H., Wu, S.C., Yu, Y.C., 2005. Geological characteristics and origin of the Xitian tin orefield in eastern Hunan Province. Geol. Miner. Resour. South China 2, 61–67 (in Chinese with English abstract).
Ma, T.Q., Wang, X.H., Bai, D.Y., 2004. Geochemical characteristics and its tectonic setting of the Xitian tungsten–tin-bearing granite pluton. Geol. Miner. Resour. South China 1, 11–16 (in Chinese with English abstract).
Ma, T.Q., Bai, D.Y., Kuang, J., Wang, X.H., 2005. Zircon SHRIMP dating of the Xitian granite pluton, Chaling, southeastern Hunan, and its geological significance. Geol. Bull. China 24, 415–419 (in Chinese with English abstract).
Mao, J.W., Li, H.Y., 1995. Evolution of the Qianlishan granite stock and its relation to the Shizhuyuan polymetallic tungsten deposit. Int. Geol. Rev. 37, 63–80.
Mao, J.W., Chen, Y.H., Wang, P.A., 1995. Geology and geochemistry of the Dashuigou tellurium deposit, western Sichuan, China. Int. Geol. Rev. 37, 526–546.
Mao, J.W., Li, H.Y., Shimazaki, H., Raimbault, L., Guy, B., 1996a. Geology and metallogeny of the Shizhuyuan skarn-greisen deposit, Hunan Province, China. Int. Geol. Rev. 38, 1020–1039.
Mao, J.W., Raimbault, L., Guy, B., Shimazaki, H., 1996b. Manganese skarn in the Shizhuyuan polymetallic tungsten deposit, Hunan province, China. Resour. Geol. 46, 1–11.
Mao, J.W., Li., H.Y., Wang, D.H., Peng, C., 1998. Ore-forming of Mesozoic polymetallic deposits in South China and its relationship with mantle plume. Bull. Mineral. Petrol. Geochem. 17, 130–132 (in Chinese with English abstract).
Mao, J.W., Zhang, Z.C., Zhang, Z.H., Du, A.D., 1999. Re–Os isotopic dating of molybdenites in the Xiaoliugou W (Mo) deposit in the northern Qilian mountains and its geological significance. Geochim. Cosmochim. Acta 63, 1815–1818.
Mao, J.W., Li, X.F., Lehmann, B., Chen, W., Lan, X.M., Wei, S.L., 2004a. ^{40}Ar–^{39}Ar dating of tin ores and related granite in Furong tin orefield, Hunan Province, and its geodynamic significance. Mineral Deposits 23, 164–175 (in Chinese with English abstract).
Mao, J.W., Xie, G.Q., Li, X.F., Zhang, C.Q., Mei, Y.X., 2004b. Mesozoic large scale mineralization and multiple lithospheric extension in South China. Earth Sci. Front. 11, 45–55 (in Chinese with English abstract).
Mao, J.W., Xie, G.Q., Guo, C.L., Chen, Y.C., 2007. Large-scale tungsten–tin mineralization in the Nanling region, South China: metallogenic ages and corresponding geodynamic processes. Acta Petrol. Sin. 23, 2329–2338 (in Chinese with English abstract).
Mao, J.W., Xie, G.Q., Guo, C.L., Yuan, S.D., C, Y.B., Chen, Y.C., 2008. Spatial-temporal distribution of Mesozoic ore deposits in South China and their metallogenic settings. Geol. J. China Univ. 14, 510–526 (in Chinese with English abstract).
Mao, J.W., Cheng, Y.B., Chen, M.H., Frangco, P., 2013a. Major types and time–space distribution of Mesozoic ore deposits in South China and their geodynamic settings. Mineral. Deposita 48, 267–294.
Mao, Z.H., Cheng, Y.B., Liu, J.J., Yuan, S.D., Wu, S.H., Xiang, X.K., Luo, X.H., 2013b. Geology and molybdenite Re–Os age of the Dahutang granite-related veinlets-disseminated tungsten ore field in the Jiangxin Province, China. Ore Geol. Rev. 53, 422–433.
McCandless, T.E., Ruiz, J., 1993. Rhenium–osmium evidence for regional mineralization in southwestern North America. Science 261, 1282–1286.
Ni, Y.J., Shan, Y.H., Wu, S.C., Nie, G.J., Zhang, X.Q., Zhu, H.F., Liang, X.Q., 2014. Emplacement Mechanism of Indosinian Dengfuxian–Xitian Granite Pluton in Eastern Hunan, South China. Geotecton. Metallog. 38, 82–93 (in Chinese with English abstract).
Niu, R., Liu, Q., Hou, Q.L., Sun, J.F., Wu, S.C., Zhang, H.Y., Guo, Q.Q., Wang, Q., 2015. Zircon U–Pb geochronology of Xitian granitic pluton in Hunan Province and its constraints on the metallogenic ages of the tungsten–tin deposit. Acta Petrol. Sin. 31, 2620–2632 (in Chinese with English abstract).
Pearce, N.J., Perkins, W.T., Westgate, J.A., Gorton, M.P., Jackson, S.E., Neal, C.R., Chenery, S.P., 1997. A compilation of new and published major and trace element data for NIST SRM 610 and NIST SRM 612 glass reference materials. Geostand. Newslett. 21, 115–144.
Peng, J.T., Zhou, M.F., Hu, R.Z., Shen, N.P., Yuan, S.D., Bi, X.W., Du, A.D., Qu, W.J., 2006. Precise molybdenite Re–Os and mica Ar–Ar dating of the Mesozoic Yaogangxian tungsten deposit, central Nanling district, South China. Mineral. Deposita 41, 661–669.
Peng, J.T., Hu, R.Z., Bi, X.W., Bai, T.M., Li, Z.L., Li, X.M., Shuang, Y., Yuan, S.D., Liu, S.R., 2007. $^{40}Ar/^{39}Ar$ isotopic dating of tin mineralization in Furong deposit of Hunan Province and its geological significance. Mineral Deposits 26, 237–248 (in Chinese with English abstract).
Peng, J.T., Hu, R.Z., Yuan, S.D., Bi, X.W., Sheng, N.P., 2008. The time ranges of granitoid emplacement and related nonferrous metallic mineralization in Southern Hunan. Geol. Rev. 54, 617–625 (in Chinese with English abstract).
Pirajno, F., Bagas, L., 2002. Gold and silver metallogeny of the South China Fold belt: a consequence of multiple mineralizing events? Ore Geol. Rev. 20, 109–126.
Qi, H.W., Hu, R.Z., Qang, X.F., Qu, W.J., Bi, X.W., Peng, J.T., 2012. Molybdenite Re–Os and muscovite $^{40}Ar/^{39}Ar$ dating of quartz vein-type W–Sn polymetallic deposits in Northern Guangdong, South China. Mineral. Deposita 47, 607–622.
Qiu, Y., Gao, S., McNaughton, N.J., Groves, D.I., Ling, W., 2000. First evidence of >3.2 Ga continental crust in the Yangtze craton of south China and its implications for Archean crustal evolution and Phanerozoic tectonic. Geology 28, 11–14.
RGNTD (Research Group for Nanling Tungsten Deposits, Chinese Ministry of Metallurgy), 1985e. Tungsten Deposits in South China. Publishing House of Metallurgical Industry, Beijing 496 pp (in Chinese with English abstract).
Rubatto, D., 2002. Zircon trace element geochemistry: partitioning with garnet and the link between U–Pb ages and metamorphism. Chem. Geol. 184, 123–138.
Ruiz, J., Mathur, R., 1999. Metallogenesis in continental margins: Re–Os evidence from porphyry copper deposits in Chile: Application of radiogenic isotopes to ore deposit research and exploration. Rev. Econ. Geol. 12, 59–72.
Selby, D., Creaser, R.A., 2004. Macroscale NTIMS and microscale LA-MC-ICP-MS Re–Os isotopic analysis of molybdenite: Testing spatial restrictions for reliable Re–Os age determinations, and implications for the decoupling of Re and Os within molybdenite. Geochim. Cosmochim. Acta 68, 3897–3908.
Selby, D., Creaser, R.A., Hart, C.J.R., Rombach, C.S., Thompson, J.F.H., Smith, M.T., Bakke, A.A., Goldfarb, R.J., 2002. Absolute timing of sulfide and gold mineralization: a comparison of Re–Os molybdenite and Ar–Ar mica methods from the Tintina Gold Belt, Alaska. Geology 30, 791–794.
Sewell, R., Campbell, S., 1997. Geochemistry of coeval Mesozoic plutonic and volcanic suites in Hong Kong. J. Geol. Soc. 154, 1053–1066.
Shirey, S.B., Walker, R.J., 1995. Carius tube digestion for low–blank rhenium–osmium analysis. Anal. Chem. 67, 2136–2141.
Smoliar, M.I., Walker, R.J., Morgan, J.W., 1996. Re–Os ages of group IIA, IIIA, IVA, and IVB iron meteorites. Science 271, 1099–1102.
Stein, H.J., Markey, R.J., Morgan, J.W., 1997. Highly Precise and Accurate Re–Os Ages for Molybdenite from the East Qinling Molybdenum Belt, Shaanxi Province, China. Econ. Geol. 92, 827–835.
Stein, H.J., Sundblad, K., Markey, R.J., Morgan, J.W., Motuza, G., 1998. Re–Os ages for Archean molybdenite and pyrite, Kuittila–Kivisuo, Finland and Proterozoic molybdenite, Kabeliai, Lithuania: testing the chronometer in a metamorphic and metasomatic setting. Mineral. Deposita 33, 329–345.
Stein, H.J., Markey, R.J., Morgan, J.W., Hannah, J.L., Scherstén, A., 2001. The remarkable Re–Os chronometer in molybdenite: how and why it works. Terra Nova 13, 479–486.
Su, H.Z., Guo, C.L., Wu, S.C., Hou, K.J., Zhang, Y., 2015. Magma-hydrothermal fluid activity duration and material sources in the Xitian Indosinian-Yanshanian complex. Acta Geol. Sin. 89, 1853–1872 (in Chinese with English abstract).
Sun, Y.L., Zhou, M.F., Sun, M., 2001. Routine Os analysis by isotope dilution–inductively coupled plasma mass spectrometry: OsO_4 in water solution gives high sensitivity. J. Anal. At. Spectrom. 16, 345–349.

Sun, T., Zhou, X.M., Chen, P.R., Li, H.M., Zhou, H.Y., Wang, Z.C., Shen, W.Z., 2003. Strongly peraluminous granites of Mesozoic in Eastern Nanling Range, southern China: Petrogenesis and implications for tectonics. Sci. China Ser. D Earth Sci. 48, 165–174 (in Chinese).

Sun, Y.L., Xu, P., Li, J., He, K., Chu, Z.Y., Wang, C.Y., 2010. A practical method for determination of molybdenite Re–Os age by inductively coupled plasma–mass spectrometry combined with Carius tube-HNO_3 digestion. Anal. Methods 2, 575–581.

Suzuki, K., Shimizu, H., Masuda, A., 1996. Re–Os dating of molybdenites from ore deposits in Japan: Implication for the closure temperature of the Re–Os system for molybdenite and the cooling history of molybdenum ore deposits. Geochim. Cosmochim. Acta 60, 3151–3159.

Tan, J., Wei, J.H., Li, Y.J., Li, Y.H., Yan, Y.F., 2007. Some reviews on diagenesis and metallogeny of the Mesozoic crustal remelting granitoids in the Nanling region. Geol. Rev. 53, 349–361 (in Chinese with English abstract).

Taylor, S.R., 1964. Abundance of chemical elements in the continental crust: a new table. Geochim. Cosmochim. Acta 28 (8), 1273–1285.

Turner, S.P., Foden, J.D., Morrison, R.S., 1992. Derivation of some A-type magmas by fractionation of basaltic magma: an example from the Padthaway Ridge, South Australia. Lithos 28, 151–179.

USGS(United States Geological Survey), 2016. Mineral Commodity Summaries, 2016. Government Printing Office (http://minerals.usgs.gov/minerals/pubs/mcs/2016/mcs2016.pdf).

Wang, Y.J., Fan, W.M., Guo, F., Peng, T.P., Li, C.W., 2003a. Geochemistry of Mesozoic Mafic Rocks Adjacent to the Chenzhou–Linwu fault, South China: Implications for the Lithospheric Boundary between the Yangtze and Cathaysia Blocks. Int. Geol. Rev. 45, 263–286.

Wang, Y.J., Fan, W.M., Guo, F., Peng, T.P., Lin, G., 2003b. Geochemistry of early Mesozoic potassium-rich diorites-granodiorites in southeastern Hunan Province, South China: petrogenesis and tectonic implications. Geochem. J. 37, 427–448.

Wang, Q., Li, J.W., Jian, P., Zhao, Z.H., Xiong, X.L., Bao, Z.W., Xü, J.F., Li, C.F., Ma, J.L., 2005. Alkaline syenites in eastern Cathaysia (South China): Link to Permian–Triassic transtension. Earth Planet. Sci. Lett. 230, 339–354.

Wang, Y.J., Fan, W.M., Sun, M., Liang, X.Q., Zhang, Y.H., Peng, T.P., 2007. Geochronological, geochemical and geothermal constraints on petrogenesis of the Indosinian peraluminous granites in the South China Block: A case study in the Hunan Province. Lithos 96, 475–502.

Wang, Y.L., Pei, R.F., Li, J.W., Qu, W.J., Li, L., Wang, H.L., Du, A.D., 2008. Re–Os dating of molybdenite from the Yaogangxian tungsten deposit, South China, and its geological significance. Acta Geol. Sin. 82, 820–825.

Wang, X.F., Qi, H.W., Hu, R.Z., Qu, W.J., Peng, J.T., Bi, X.W., 2010a. Re–Os isotopic chronology of molybdenites from Hongling tungsten deposit of Guangdong province and its geological significance. Mineral Deposits 29, 415–427 (in Chinese with English abstract).

Wang, Y.J., Zhang, F.F., Fan, W.M., Zhang, G.W., Chen, S.Y., Cawood, P.A., Zhang, A.M., 2010b. Tectonic setting of the South China Block in the early Paleozoic: Resolving intracontinental and ocean closure models from detrital zircon U–Pb geochronology. Tectonics 29, 1–16.

Wang, F.Y., Li, C.Y., Ling, M.X., Zhang, H., Sun, Y.L., Sun, W.D., 2011a. Geochronology of the Xihuashan tungsten deposit in Southeastern China: Constraints from Re–Os and U–Pb dating. Resour. Geol. 61, 414–423.

Wang, L., Hu, M., Yang, Z., Qu, W., Xia, J., Chen, K., 2011b. U–pb and Re–Os geochronology and geodynamic setting of the Dabaoshan polymetallic deposti, northern Guangdong Province, South China. Ore Geol. Rev. 43, 40–49.

Wang, M., Bai, X.J., Hu, R.G., Cheng, S.B., Pu, Z.P., Qiu, H.N., 2015. Direct dating of cassiterite in Xitian tungsten-tin polymetallic depoist, southeastern Hunan, by $^{40}Ar/^{39}Ar$ progressive crushing. Geotecton. Metallog. 12, 1049–1060 (in Chinese with English abstract).

Wei, D.F., Bao, Z.Y., Fu, J.M., Cai, M.H., 2007. Diagenetic and mineralization age of the Hehuaping tin-polymetallic orefield, Hunan Province. Acta Geol. Sin. 81, 244–252.

Whalen, J.B., Currie, K.L., Chappell, B.W., 1987. A-type granites: geochemical characteristics, discrimination and petrogenesis. Contrib. Mineral. Petrol. 95, 407–419.

Wu, S.C., Luo, H.W., Huang, T., 2004. Metallogenetic geological characteristcs and prospecting of tin polymetallic deposits in central Xitian area, easeren Hunan Province. Geol. Miner. Resour. South China 2, 21–27 (in Chinese with English abstract).

Wu, L.Y., Hu, R.Z., Peng, J.T., Bi, W.X., Jiang, G.H., Chen, H.W., Wang, Q.Y., Liu, Y.Y., 2011. He and Ar isotopic compositions and genetic implications for the giant Shizhuyuan W–Sn–Bi–Mo deposit, Hunan Province, South China. Int. Geol. Rev. 53, 677–690.

Wu, S.C., Long, Z.Q., Xu, H.H., Zhou, Y., Jiang, Y., Pan, C.C., 2012. Structural characteristics and prospecting significance of the Xitian tin–tungsten polymetallic deposit, Hunan Province, China. Geotecton. Metallog. 36, 217–226 (in Chinese with English abstract).

Xu, H.H., Wu, S.C., Yu, Y.C., Xie, Y.L., Long, W.P., 2006. Geological characteristics and ore-controlling factors of Xitian skarn-type W–Sn Deposit in Hunan Province. Geol. Miner. Resour. South China 2, 37–42 (in Chinese with English abstract).

Yang, X.J., Wu, S.C., Fu, J.M., Huang, H.L., Chang, H.L., Liu, Y.H., Wei, J.Q., Liu, G.Q., Ma, L.Y., 2007. Fluid inclusion studies of Longshang tin-polymetallic deposit in Xitian ore field, eastern Hunan Province. Mineral Deposits 26, 501–512 (in Chinese with English abstract).

Yang, F., Li, X.F., Feng, Z.H., Bai, Y.P., 2009a. $^{40}Ar/^{39}Ar$ dating of muscovite from greisenized granite and geological significance in Limu tin deposit. J. Guilin Univ. Technol. 29, 21–24 (in Chinese with English abatract).

Yang, J.H., Chen, X.Y., Wang, X.D., 2009b. Zircon LA-ICPMS U–Pb dating and ore-forming fluid geochemical characteristics of Dangping tungsten-bearing granites in Jiangxi province, Southeast China. Acta Mineral. Sin. 29, 339–340 (in Chinese with English abstract).

Yao, J.M., Hua, R.M., Liu, J.F., 2005. Zircon LA-ICPMS U–Pb dating and geochemical characteristics of Huangshaping granite in southeast Hunan province, China. Acta Petrol. Sin. 21, 688–696 (in Chinese with English abstract).

Yao, J.M., Hua, R.M., Qu, Q.J., Qi, H.W., Lin, J.F., Du, A.D., 2007. Re–Os isotope dating of molybdenites in the Huangshaping Pb–Zn–W–Mo polymetallic deposit, Hunan Province, South China and its geological significance. Sci. China Ser. D Earth Sci. 50, 519–526 (in Chinese).

Yao, Y., Chen, J., Lu, J., Zhang, R., 2013. Geochronology, Hf isotopic compositions and geochemical characteristics of Xitian A-type granite and its geological significance. Mineral Deposits 32, 467–488 (In Chinese with English abstract).

Yin, J., Kim, S.J., Lee, H.K., Itaya, T., 2002. K–Ar ages of plutonism and mineralisation at the Shizhuyuan W–Sn–Bi–Mo deposit, Hunan Province, China. J. Asian Earth Sci. 20, 151–155.

Yu, J.J., Mao, J.W., 2004. $^{40}Ar–^{39}Ar$ dating of albite and phlogopite from porphyry iron deposits in the Ningwu Basin in east-centralat China and its the Shizhuyuan W–Sn–Bisignificance. Acta Geol. Sin. 78, 435–442.

Yu, J.H., Wang, L.J., O'Reilly, S.Y., Griffin, W.L., Zhang, M., Li, C.Z., Shu, L.S., 2009. A Paleoproterozoic orogeny recorded in a long–lived cratonic remnant (Wuyishan terrane), eastern Cathaysia block, China. Precambrian Res. 174, 347–363.

Yuan, S.D., Peng, J.T., Shen, N.P., Hu, R.Z., Dai, T.M., 2007. $^{40}Ar–^{39}Ar$ isotopic dating of the Xianghualing Sn-polymetallic orefiedl in Southern Hunan, China and its geological implications. Acta Geol. Sin. 81, 278–286 (in Chinese with English abstract).

Yuan, S.D., Zhang, D.L., Shuang, Y., Du, A.D., Qu, W.J., 2012. Re–Os dating of molybdenite from the Xintianling giant tungsten–molybdenum deposit in southern Hunan Province, China and its geological implications. Acta Petrol. Sin. 28, 27–38 (in Chinese with English abstract).

Zaw, K., Peters, S.G., Cromie, P., Burrett, C., Hou, Z.Q., 2007. Nature, diversity of deposit types and metallogenic relations of South China. Ore Geol. Rev. 31, 3–47.

Zeng, G.H., Hu, Y.Z., Yu, Y.C., 2005. Geological characteristics and prospecting potential of the Longshang skarn tin-polymetallic deposit in Xitian orefield, eastern Hunan Province. Geol. Miner. Resour. South China 2, 68–72 (in Chinese with English abstract).

Zeng, Z.L., Zhang, Y.Z., Zhu, X.P., Chen, Z.H., Wang, C.H., Qu, W.J., 2009. Re–Os isotopic dating of molybdenite from the Maoping tungsten–tin deposit in Chongyi County of Southern Jiangxi Province and its geological significance. Rock Miner. Anal. 28, 209–214 (in Chinese with English abstract).

Zhai, W., Sun, X.M., Wu, Y.S., Sun, H.Y., Hua, R.M., Yang, Y.Q., Li, W.Q., Li, S.H., 2010. Zircon SHRIMP U–Pb dating of the buried granodiorite and muscovite $^{40}Ar/^{39}Ar$ dating of mineralization and geological implications of Meiziwo tungsten deposit, northern Guangdong Province, China. Geol. J. China Univ. 16, 177–185 (in Chinese with English abstract).

Zhang, L.C., Xiao, W.J., Qin, K.Z., Qu, W.J., Du, A.D., 2004. Re–Os isotopic dating of molybdenite and pyrite in the Baishan Mo–Re deposit, eastern Tianshan, NW China, and its geological significance. Mineral. Deposita 39, 960–969.

Zhang, W.L., Hua, R.M., Wang, R.C., Chen, P.R., Li, H.M., 2006. New dating of the Dajishan granite and related tungsten mineralization in Southern Jiangxi. Acta Geol. Sin. 80, 956–962 (in Chinese with English abstract).

Zhang, W.L., Hua, R.M., Wang, R.C., Li, H.M., Qu, W.J., Ji, J.Q., 2009. New dating of the Piaotang granite and related tungsten mineralization in Southern Jiangxi. Acta Geol. Sin. 83, 659–670 (in Chinese with English abstract).

Zhao, J.H., Zhou, M.F., Yan, D.P., Zheng, J.P., Li, J.W., 2011. Reappraisal of the ages of Neoproterozoic strata in South China: No connection with the Grenvillian orogeny. Geology 39, 299–302.

Zhou, X.M., Li, W.X., 2000. Origin of Late Mesozoic igneous rocks in Southeastern China: implications for lithosphere subduction and underplating of mafic magmas. Tectonophysics 326, 269–287.

Zhou, X.M., Sun, T., Shen, W.Z., 2006. Petrogenesis of Mesozoic granitoids and volcanic rocks in South China: A response to tectonic evolution. Episodes 29, 26–33.

Zhou, Y., Liang, X.Q., Liang, X.R., Wu, S.C., Jiang, Y., Wen, S.N., Cai, Y.F., 2013. Geochronology and geochemical characteristics of the Xitian tungsen–tin- bearing A-type granite, Hunan Province, China. Geotecton. Metallog. 37, 517–535 (in Chinese with English abstract).

Zhou, Y., Liang, X.Q., Wu, S.C., Cai, Y.F., Liang, X.R., Shao, T.B., Wang, C., Fu, J.G., Jiang, Y., 2015. Isotopic geochemistry, zircon U–Pb ages and Hf isotopes of A-type granites from the Xitian W–Sn deposit, SE China: Constraints on petrogenesis and tectonic significance. J. Asian Earth Sci. 105, 122–139.

Zhu, J.C., Xie, C.F., Zhang, P.H., Yang, C., Gu, C.Y., 2005. Niutiao and Tong'an intrusive bodies of NE Guangxi: Petrology, zircon SHRIMP U–Pb geochronology and geochemistry. Acta Petrol. Sin. 21, 665–676 (in Chinese with English abstract).

Zou, X.W., Cui, S., Qu, W.J., Bai, Y.S., Chen, X.Q., 2009. Re–Os isotope dating of the Liguifu tungsten–tin polymetallic deposit in Dupangling area, Guangxi. Geol. China 36, 837–844 (in Chinese with English abstract).